Design and building of a new experimental setup for testing hydrogen storage materials

Andreasen, A.

Publication date:
2005

Document Version
Publisher's PDF, also known as Version of record

RISØ

Risø-R-1531(EN)

Design and building of a new experimental setup for testing hydrogen storage materials

Anders Andreasen

Materials Research Department

Risø National Laboratory
Roskilde
Denmark
September 2005

Risø-R Report

Author: Anders Andreasen
Title: Design and building of a new experimental setup for testing hydrogen storage materials
Department: Materials Research Department

Abstract:
For hydrogen to become the future energy carrier a suitable way of storing hydrogen is needed, especially if hydrogen is to be used in mobile applications such as cars. To test potential hydrogen storage materials with respect to capacity, kinetics and thermodynamics the Materials Research Department has a high pressure balance. However, the drawback of this equipment is, that in order to load samples, exposure towards air is inevitable. This has prompted the design and building of a new experimental setup with a detachable reactor allowing samples to be loaded under protective atmosphere. The purpose of this report is to serve as documentation of the new setup.

Risø-R-1531(EN)
September 2005

ISSN 0106-2840
ISBN 87-550-3470-5

Contract no.:

Group's own reg. no.:
1625049-00

Sponsorship:

Cover :

Pages: 52
Tables: 13
References: 23

Risø National Laboratory
Information Service Department
P.O.Box 49
DK-4000 Roskilde
Denmark
Telephone +45 46774004
bibl@risoe.dk
Fax +45 46774013
www.risoe.dk

Contents

1 Introduction

1.1 The purpose of this report

The main purpose of this report is to describe a new experimental setup in the Materials Research Department, Risø National Laboratory for testing hydrogen storage materials. This report is thought of as a documentation of the design and principles of operation of the setup, respectively, including a description of all the subparts of the setup, an evaluation of the performance of the setup, and a discussion of possible experimental errors. This report is not intended as a step-by-step operations manual. During preparation of this report emphasis have been put on technical information rather than readability.

1.2 Towards the hydrogen based society

A growing interest in the transformation of the hydrocarbon based society into a hydrogen based society is emerging around the world. This is induced by the fact that hydrogen offer some key advantages compared to hydrocarbons: Produced by electrolysis of water using renewable energy sources e.g. solar, wind or water power as a source of electricity the need for hydrocarbons is greatly reduced. Further, converting the chemically stored energy in H_2 to electricity in a fuel cell under the right conditions water is the only combustion product.

However, for the hydrocarbon based society to become realizable a suitable way of storing hydrogen in between the production and the use of hydrogen must be offered. This is indeed a problem that needs special attention if hydrogen should become the future choice of energy source in mobile applications e.g. cars due to the very specific demands for safety, volumetric energy density, gravimetric energy density etc. [1]. Different ways of storing hydrogen exist e.g storage in high pressure cylinders, storage as liquid hydrogen, physisorption in carbon nanotubes and storage in metal hydrides [2]. In our view the storage of hydrogen in metal hydrides is perhaps the most interesting and challenging [3].

1.3 Hydrogen storage in metals

Storage of hydrogen in metal hydrides is possible since many metals react readily with hydrogen forming a stable metal hydride. For instance, Mg reacts with hydrogen forming a hydride of the form MgH_2. Thus, storing 7.6 wt. % of hydrogen and thereby fulfilling the gravimetric hydrogen density criterion suggested by the U.S. Department of Energy for year 2010 [1] for on-board storage in mobile applications. However, in order to release hydrogen at a pressure of 1 bar the hydride must be heated to above 280 °C. This is because magnesium forms a (too) stable hydride with a heat of formation of approx. ΔH_f=75 kJ/mol. In the future it is imagined that the traditional combustion engine with efficiency limited by the Carnot cycle will be replaced by a PEM fuel cell. A car driven by a PEM fuel cell operated at around 80-100 °C is not capable of supplying the required heat for this operation (in fact 100 °C is the upper operable temperature limit for metal hydrides suggested by USDOE [4]). Alternatively, the hydride bed may be heated by combustion of hydrogen. This will however lower the efficiency by approx. 25 % [2]. Another way around this problem is to use another hydride material with improved thermodynamical properties e.g. $LaNi_5$ or FeTi which deliver hydrogen at tempeartures as low as 12 °C and -8 °C. These materials do however fail to meet the gravimetric energy density criterion since they store only 1.5 wt. % and 1.85 wt. % of hydrogen, respectively [2].

[1] U. S. Department of Energy, `http://www.eere.energy.gov/hydrogenandfuelcells/hydrogen/-storage.html` Last checked April 2004.

[2] Hydride Information Center, Sandia National Laboratories, `http://hydpark.ca.sandia.gov`, Last checked april 2004.

1.4 Contributors

Besides the author of this report the following people have contributed to the design and building of the experimental setup described in this report:

Mike Wichmann Research Technician, Materials Research Department, Risoe National Laboratory, Frederiksborgvej 399, DK-4000 Roskilde, Denmark.
E-mail:mike.wichmann@risoe.dk

Allan Schrøder Pedersen Supervisor, Senior scientist, Deputy head of department, Materials Research Department, Risoe National Laboratory, Frederiksborgvej 399, DK-4000 Roskilde, Denmark.
E-mail:allan.schroeder.pedersen@risoe.dk

Further, Research Technician Ole Olsen and Research Technician John Kjøller (both retired), Materials Research Department, Risoe National Laboratory, Frederiksborgvej 399, DK-4000 Roskilde, Denmark, have also contributed in the early design stage.

1.5 Outline

Section 2 In this section some concepts often used when discussing hydrogen storage in metal hydrides are briefly reviewed.

Section 3 describes the existing setup at Risø for testing hydrogen storage materials.

Section 4 is a general description of the new setup at Risø. Keywords: design criterion, principle of operation, expansion of known volumes, calculating hydrogen uptake etc.

Section 5 is a more detailed description of all the subparts (hardware) of the experimental setup.

Section 6 is a description of the LabView software used for data acquisition and the post processing of the data using GNU/Octave.

Section 7. In this section the performance of the setup is evaluated with respect to leak integrity, temperature control, determination of hydrogen capacity and kinetics, respectively.

2 Concepts

In order for a metal hydride to be of practical interest for hydrogen storage applications it should fulfill the following:

Capacity: The metal hydride should contain a sufficient amount of hydrogen. For on-board storage in mobile applications the target set by the International Energy Agency (IEA) Hydrogen program Task 17 is gravimetric hydrogen density of 5 wt. %[3].

Kinetics: Fast take up (hydrogenation) and release (dehydrogenation) of hydrogen. The target set by the U.S. Department of Energy (USDOE), The Hydrogen, Fuel Cells & Infrastructure Technologies Program the refueling should not exceed 3 min.[4]

Thermodynamics: The hydride should not require *too* high a temperature in order to release hydrogen. The target set by IEA is a hydrogen desorption pressure of 1 bar at 80 °C (see footnote 3).

Stability: The capacity and kinetics should remain unchanged even over several cycles of hydrogenation/dehydrogenation. The USDOE target is a lifetime exceeding 1500 cycles (see footnote 4).

More specific targets can be found at the U.S. Department of energy website (see footnote 4).

2.1 The hydrogen-metal reaction

The reaction of hydrogen with a metal or an intermetallic compound can be described by the following equation:

$$Me(s) + \frac{x}{2}H_2(g) \rightleftharpoons MeH_x(s) \quad (1)$$

This is of course a simplified picture. A more detailed picture is shown in figure 1. Hydrogen adsorbs and dissociates at the surface of the metal and penetrates into the bulk forming a solid solution of hydrogen in the metal host lattice also denoted the α-phase. At higher hydrogen contents a hydride phase is formed (MeH_x) also denoted the β-phase.

2.2 Capacity

The hydrogen capacity or uptake may be defined in a variety of different ways:

H/M This notation gives the ratio of total number of hydrogen absorbed by the sample per total number of moles metal atoms e.g. $LaNi_5H_6$ has a H/M ratio of 1. H/M ratios often encountered are integer values 1,2 and sometimes 3. However, non integer values also appear e.g. Mg_2NiH_4.

Gravimetric hydrogen density Also denoted ρ_m, is the ratio between the weight of hydrogen and the weight of the hydride. ρ_m is often expressed in %.

Volumetric hydrogen density Also denoted ρ_v, is the weight of hydrogen divided by the volume of the hydride often expressed in kg/m^3.

Reacted fraction Also denoted α. $\alpha = 0$ corresponds to the pure unreacted metal and $\alpha = 1$ corresponds to the fully reacted hydride. Thus, α does not explicitly tell the amount of hydrogen taken up.

[3] http://www.eere.energy.gov/hydrogenandfuelcells/hydrogen/iea/tasks/task17.html
[4] http://www.eere.energy.gov/hydrogenandfuelcells/hydrogen/storage.html

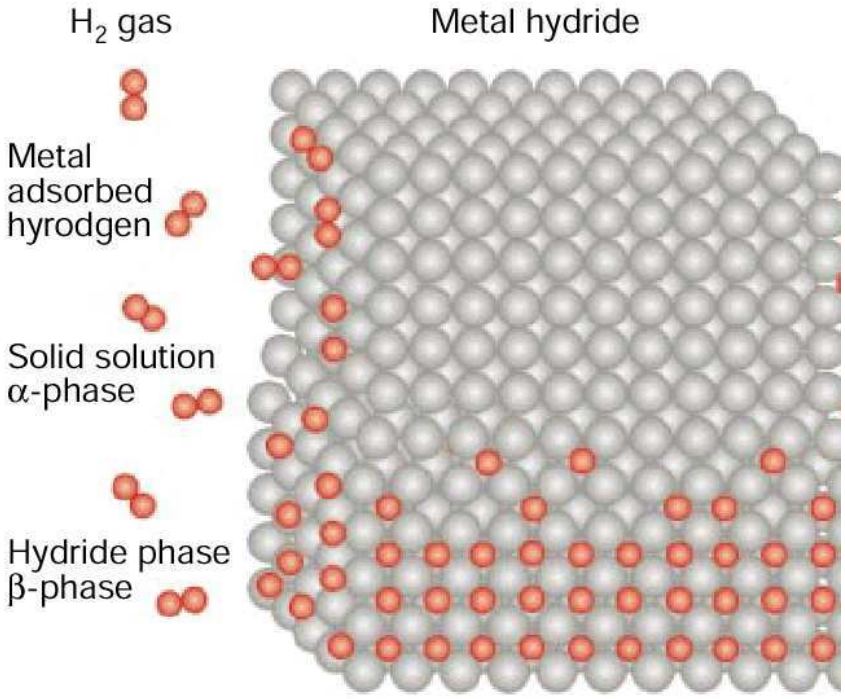

Figure 1: Interaction of gaseous hydrogen with a metal or intermetallic host lattice forming a metal hydride. Adapted from ref. [1].

2.3 Kinetics

Kinetics may be described as the time dependent uptake (or release) of hydrogen. While the capacity is a stationary quantity (equilibrium) where the net rate of reaction is zero, kinetics describes the dynamics (where the net reaction rate is non-zero). The rate of reaction is often expressed as the derivative of α with respect to time. Gas-solid reactions are often described by an equation of the following form:

$$\alpha(t) = 1 - \exp\left(-(kt)^n\right) \tag{2}$$

Different types of kinetics is sketched in figure 2, where both the reacted fraction and the reaction rate is plotted against time. The figure illustrate two different kinds of kinetics often met: 1. order like reaction, where the initial rate is high and monotonically declining and the sigmodal shaped reacted fraction (nucleation and growth type), where the initial rate is low and goes through a maximum at $\alpha = 0.5$. Assuming that the rate constant k is described by an Arrhenius relation:

$$k = A \exp\left(-\frac{E_a}{RT}\right) \tag{3}$$

the activation energy,E_a, may be determined by measurements of α vs. time for various temperatures, fitting k in the rate equation and plotting ln(k) vs. reciprocal temperature. The activation energy is then determined from the slope.

2.4 Thermodynamics

A very useful tool in describing the thermodynamics of a metal-hydrogen system is the Pressure Composition Isotherm (PCI) cf. figure 3. The PCI is constructed by measuring the equilib-

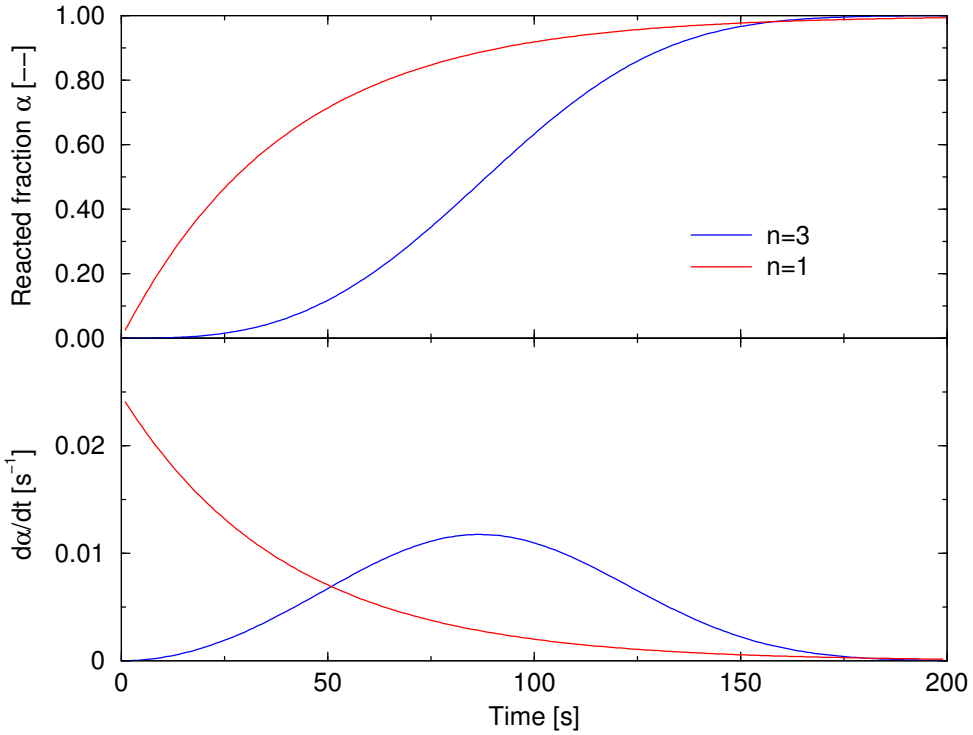

Figure 2: Reacted fraction (upper) and reaction rate (lower) as a function of time for 1. (red) and 3. order (blue) kinetics, respectively.

rium uptake as function of applied hydrogen pressure at isothermal conditions and plotting the transpose. When the hydrogen pressure initially is increased, only a relatively small amount of hydrogen is absorbed. This is a solid solution of hydrogen (α-phase). Increasing the pressure further will result in the formation of the β-phase and a small increase in pressure results in a large uptake. This gives rise to a plateau where the pressure is more or less the same (plateau pressure or $p_{h_2}^{eq}$) but with large variations in the hydrogen content. The width of the plateau gives the reversible storage capacity. In this region the α- and the β-phase co-exist. Increasing the hydrogen pressure further leads to a solid solution of hydrogen in β-phase, resulting in only little further uptake. Drawing PCI at different temperature the phase diagram can be constructed (dashed line).

At equilibrium the following relation holds:

$$K = \exp\left(-\frac{\Delta G}{RT}\right) \tag{4}$$

where K is the equilibrium constant for metal-hydrogen reaction (eq. 1). This can be rewritten as:

$$\ln\left(\frac{p_{H_2}^{eq}}{p^{\ominus}}\right) = \frac{\Delta H}{RT} - \frac{\Delta S}{R} \tag{5}$$

Plotting the experimentally observed plateau pressures as a function of reciprocal temperature will yield a straight line from which the reaction enthalpy and the entropy may be determined from the slope and the intercept, respectively.

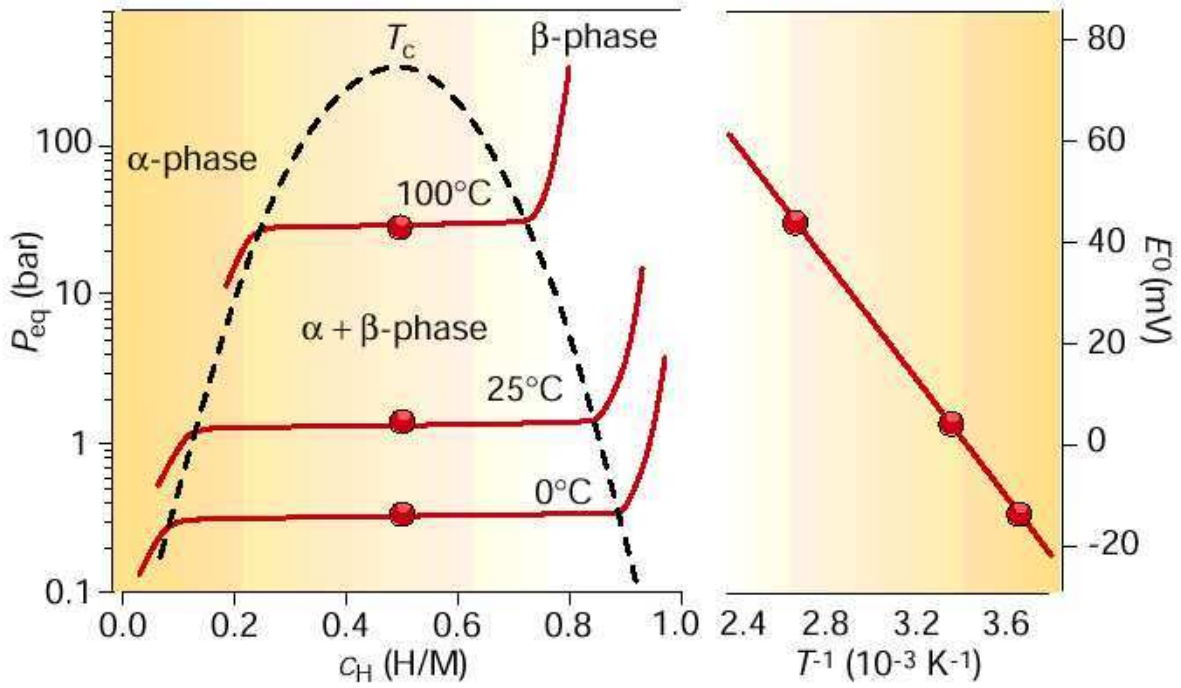

Figure 3: Left: Pressure Composition Isotherm (PCI) for $LaNi_5/LaNi_5H_6$, Right: The corresponding Van't Hoff plot derived from the plateau pressures in the PCI. Adapted from ref. [1].

2.5 Summary

Being able to measure the hydrogen uptake in a metal/intermetallic one can obtain useful information about the nature of the hydrogen interaction with the metal: *i)* Capacity i.e. the maximum uptake of hydrogen, *ii)* Kinetics. Qualitative information about the reaction mechanism may be determined from plots of α vs. time. The *apparent* activation energy can be derived from series of isothermal experiments. *iii)* Thermodynamic information i.e. ΔH, ΔS can be derived from PCI's in a Van't Hoff plot and the hydrogen solubility and reversible storage capacity may also be determined from PCI's.

3 Existing setup

3.1 Outline

The materials research department at Risø already has equipment available for testing hydrogen storage materials. The existing setup is shown in figure 4.

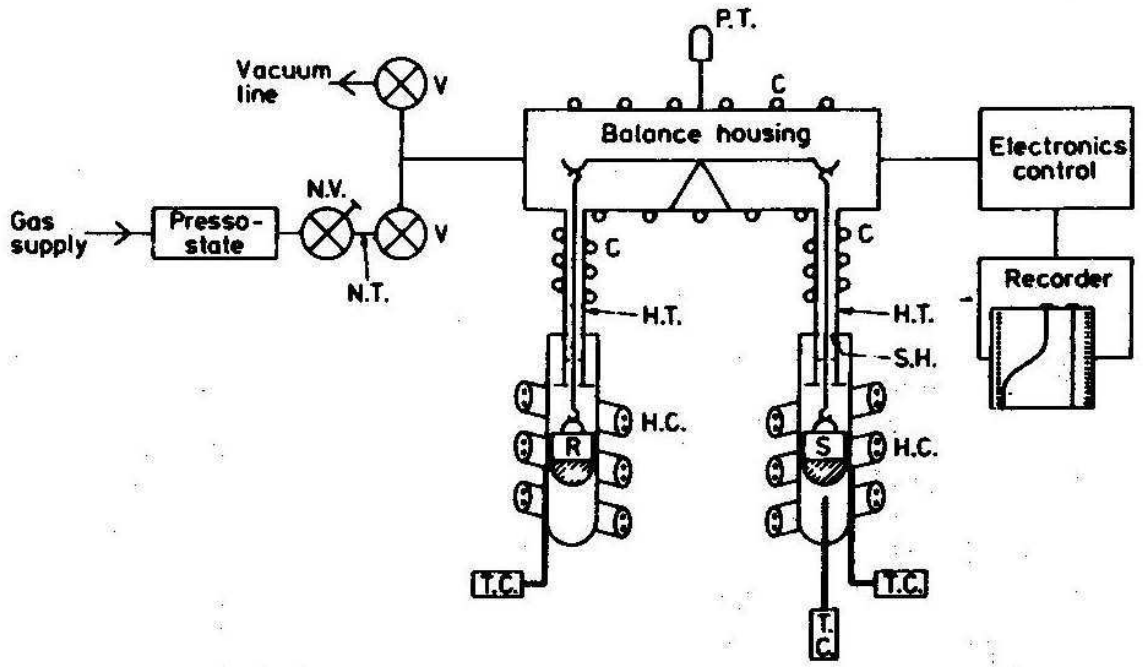

Figure 4: Existing setup for testing hydrogen storage materials. C: Cooling circuit, HC: Heating coil, HT: High pressure tubing (15 MPa), PT: Pressure transducers (piezoresistive), R: Reference (counter weight), S: Sample, SH: Shield, TC: Thermo-couple. The drawing is reproduced from ref. [5].

The core of the system is a *Sartorius* 4436 MP8 electronic micro balance for high pressure applications including the balance housing, control amplifier and display. The balance is equipped with a gas supply system (Hydrogen and Helium), an evacuation system consisting of a turbo molecular pump backed up by a roughing pump, a liquid cooling system, an oven system and a data acquisition system (weight, pressure and temperature).

3.2 Principle of operation

A sample of approx. 200-300 mg is loaded in the sample stainless steel crucible. An inert reference (i.e. not reactive towards hydrogen) with a weight +/- 1 mg of the sample of investigation is loaded into the reference crucible. To avoid buoyancy the volume of the sample and the reference should be similar and at best the same. Steel cylinders are mounted around the sample and the reference, respectively, and the system is evacuated to approx. 10^{-3} mbar and refilled with 1.5 bar of helium. This procedure is repeated 2-3 times to reduce the amount of impurities such as oxygen, water etc. that may potentially contaminate the sample. The system is subsequently heated to the desired temperature. When the reaction temperature is reached the system is evacuated and refilled with hydrogen. This defines the start of the hydrogen uptake. The advantage of the system is that the uptake of hydrogen is determined directly from

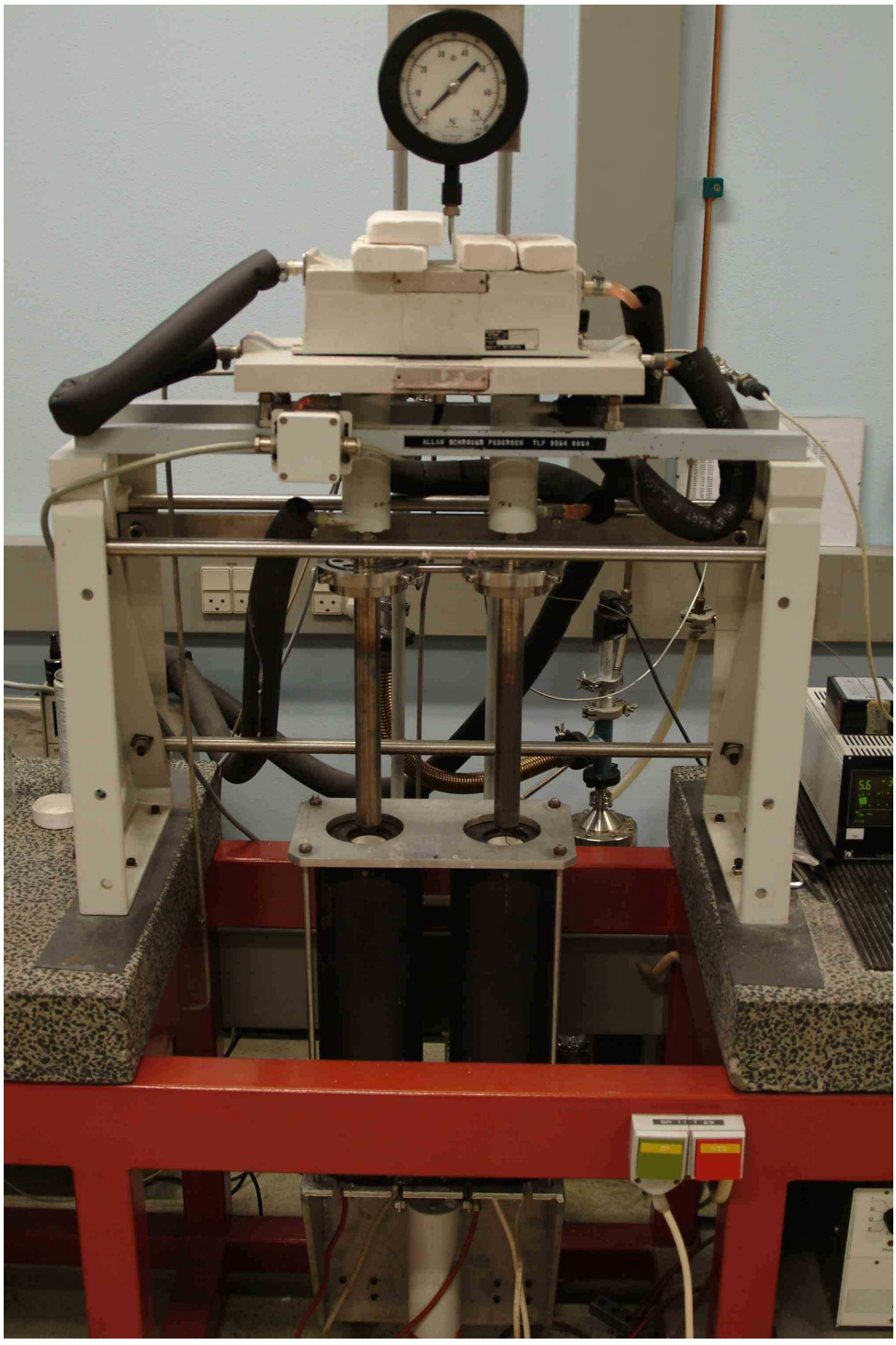

Figure 5: Existing setup for testing hydrogen storage materials.

the weight difference between the sample and the reference. Furthermore, problems regarding determination of gas amounts from measurements of pressure in known volumes such as leaks, thermal expansion, thermal gradients, adiabatic expansion etc. is eliminated. The main disadvantage is the fact that it is impossible to load the sample without exposing it to air. This is a severe problem since most materials that are reactive towards hydrogen also readily reacts with oxygen, water etc. Furthermore, direct measurement of the sample temperature with a thermocouple is impossible since this would interfere with the weight measurement.

3.3 Specifications

See table 3.3

Micro balance:	Sartorius 4406
Max.load	25 g
Ranges	10, 100 and 1000 mg
Precision	1, 10 and 100 μg
Sensitivity	< 5, 10 and 100 μg
Zero point stab.	$< 5\mu g$
Output	0-1 V
Temperature range	0-600 °C
Pressure range	0-15 MPa
Oven system:	Linseis L 70/102
Control	Programmable PID
Programs	Const. temp., linear heating/cooling
	ramp to const. temp.
Heating rates	0.1, 0.2, 0.5, 1, 2, 5, 10, 20 and 50 °C/min.
Max. deviation	6 °C
Offset	< 2 °C
Pressure measurement	Koestler Piezoresistive transducer type 4043
Range	0-5 MPa
Precision	< 0.5% of full scale
Output	0-1 V, 0-10 V and 0-20 mA
Vacuum system	

Table 1: Technical specifications of the high pressure balance system.

3.4 Example experiments

In figure 6 real PCI's are shown for $LaNi_5$ determined at 3 temperatures for hydrogenation and dehydrogenation, respectively. The PCI clearly demonstrates that for real systems hysteresis and sloping plateaus also comes into play. However this is beyond the scope of the present work. Also shown is the derived Van't Hoff plot. From this ΔH_f for hydrogenation of $LaNi_5H_x$ is found to be equal to -31.1 kJ/mol H_2 in agreement with the literature [6].

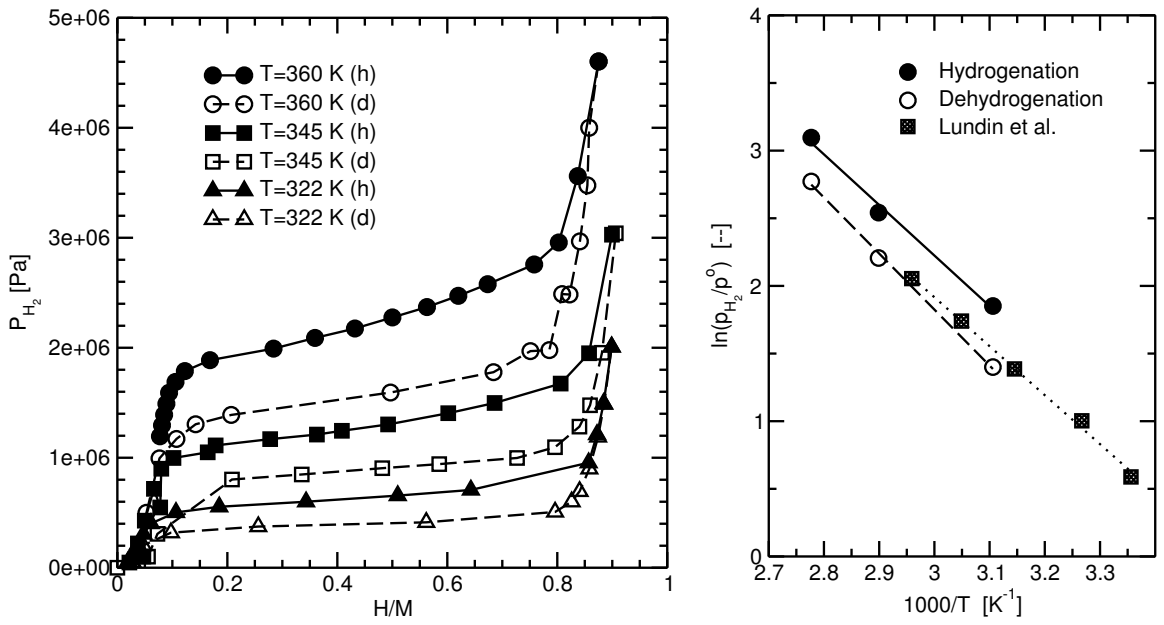

Figure 6: Left: Pressure-Composition-Isotherms (PCI) for $LaNi_5$. Right: Van't Hoff plot measured pressures at plateau midpoints (H/M=0.5) from the PCI's. The Van't Hoff plot of Lundin et al. is from ref. [6].

Experimental results based on the high pressure balance have been published in international journals. See ref. [7, 8, 9, 10, 11].

3.5 Limitations

3.5.1 Protective atmosphere

Most materials that react readily with hydrogen is also often reactive towards gas impurities such as e.g. oxygen and water vapor especially high surface area materials (e.g. ball milled materials). This will lead to either the formation of an oxide layer on metal particles or the destruction of materials. The formation of an oxide layer may effect the rate of hydrogen uptake severely e.g. when magnesium is contaminated by oxygen the activation barrier for hydrogenation/dehydrogenation is increased by almost 200 kJ/mol. Destructive contamination of samples may make it difficult to characterize the sample since important features may be lost. Further, the *new* promising class of hydrogen storage materials the complex hydrides e.g. $NaAlH_4$[12] and $LiBH_4$[13] are all hydroscopic in nature. For this reason it is highly desirable to avoid exposure of samples towards air during handling. However, during loading/unloading of samples in the existing setup this can not be avoided. At best the sample will be exposed to air for at least 5 min during loading. This is the main motivation for building a new setup which features handling of samples in protective atmosphere.

4 New setup

4.1 Design criterion

In the following the design criterion for the new setup are listed

Environment. The setup should allow loading and unloading of samples in a protective atmosphere to avoid air exposure as discussed in the previous section.

Pressure. The pressure range should be from vacuum level (10^{-2} mbar) to 100 bar. By repeatedly flushing with either hydrogen or inert (e.g. helium) with max. 1 ppm impurities and evacuating to vacuum level an impurity level of 1 ppm is within reach within a few cycles of flushing and evacuation. $NaAlH_4$ which is among the promising new complex hydrides require relatively high pressure for hydrogenation (approx. 70 bar at 150 °C [14].)

Temperature. The temperature range should be from room temperature to 500 °C. The upper limit ensures that stable hydrides such magnesium hydride, $KAlH_4$ [15], and $LiBH_4$ [13] where hydrogen desorption only occurs at elevated temperatures can be studied. The lower limit allows the study of thermodynamically less stable hydrides similar to $LaNi_5$ where hydrogen desorption is possible at ambient conditions.

Principle of measurement. The setup should feature determination of hydrogen uptake/desorption by measuring pressure changes in containers with known volume. The sensitivity of the setup should correspond to a pressure change of 10 bar upon hydrogenation (of a 5 g sample of Mg or 20 g $LaNi_5$). The pressure change upon desorption should be approx. 1 bar for the same sample. The volume of the system should be chosen to fulfill this.

4.2 Outline

The setup is depicted in figure 7 with additional details of the oven/reactor system shown in figure 8. A diagram of the setup is shown in figure 9. The reactor is a stainless steel tube which is connected to the rest of the system through a ball valve. The oven is mounted on a set of rails to allow dismounting of the reactor. The reactor can be separated from the system by unwinding the nut on the left side of the valve. The reactor can then be transported to a glove box with an inert atmosphere where it can be loaded with material. By closing the valve the reactor can be transported from the glove box to the setup without intervening air exposure of the sample. Once mounted the rest of the system is thoroughly evacuated/flushed with gas repeatedly and finally the reactor valve can be opened. Evacuation of the system is done by a rotary vacuum pump and to avoid oil vapor and residual hydrogen gas in the lab the exhaust of the pump is sent outside the building through a vent pipe. Gas (hydrogen and helium) is supplied through reduction valves, and back-flow preventers. The setup includes two gas containers: a high pressure gas container (vertically mounted cylinder from now on denoted HP) for hydrogen uptake measurements and a larger low pressure container (horizontally mounted cylinder from now on denoted LP) for hydrogen desorption measurements. During hydrogen uptake the pressure in the reactor can be controlled by a pressure controller (from now on denoted PC). During desorption the PC is bypassed. The pressure sensors in HP and LP is connected to a data acquisition system likewise is the reactor temperature sensor. The reactor temperature is controlled by a temperature sensor/controller circuit integrated in the oven.

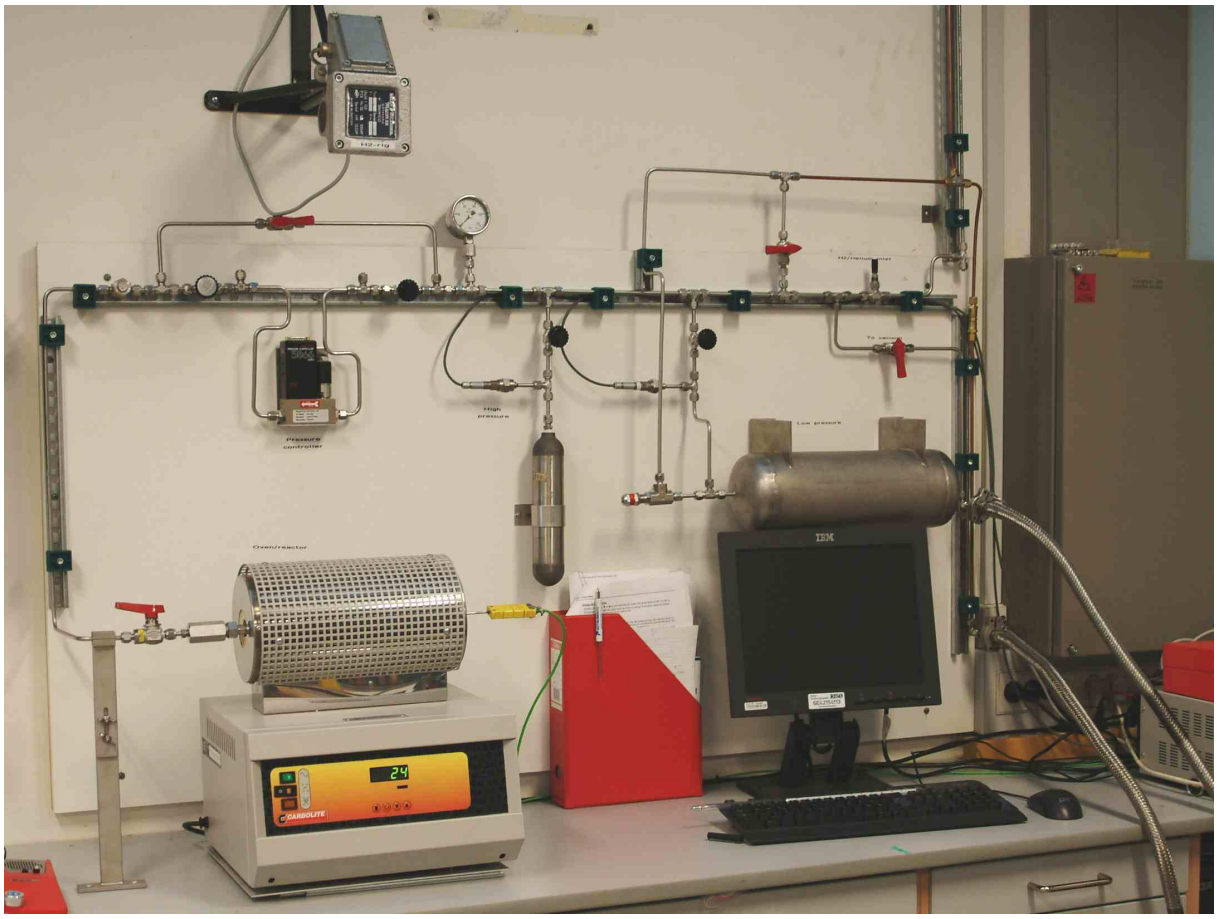

Figure 7: Picture of the new setup for testing hydrogen storage materials.

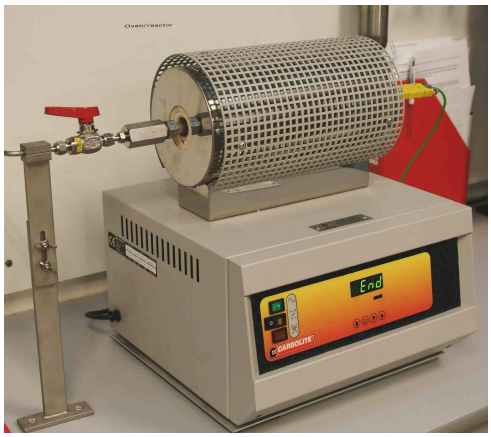

Figure 8: Picture of the reactor/oven part of the setup.

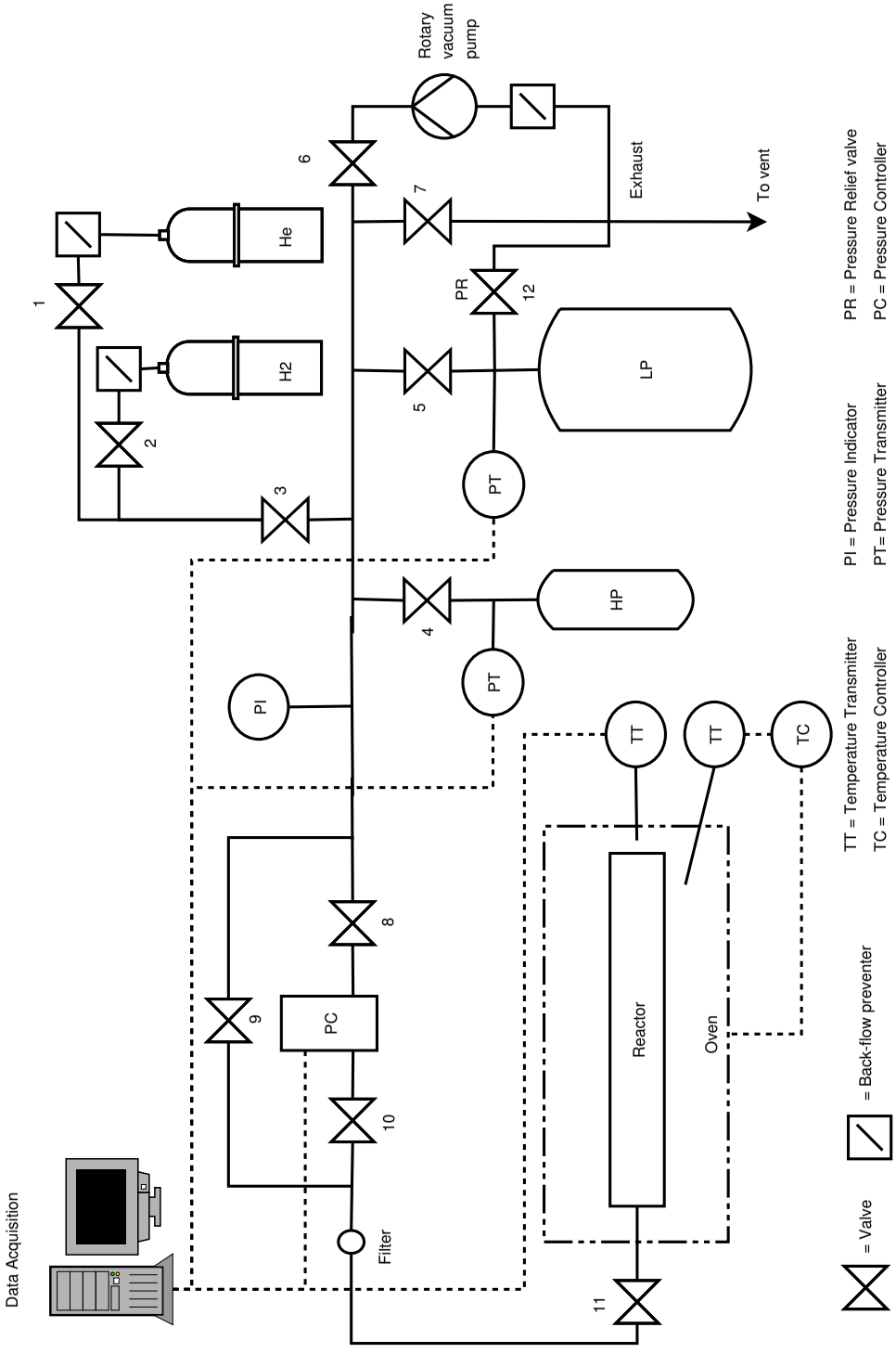

Figure 9: Diagram of the experimental setup. Full lines illustrate piping and dashed lines represent electrical connections. The dash-dotted lines illustrates the oven.

4.3 Principle of operation

4.3.1 Hydrogenation

Once the reactor with sample is connected to the system (but still with valve 11 closed) the rest of the system is evacuated and flushed with helium repeatedly since air have been introduced at least up to valve 9 and 10 during disconnection of the reactor. This is done by opening all valves except 1,2 an 7 (further if both HP and LP are *clean* the process may be speeded up by keeping valve 4 and 5 closed) and pumping down to vacuum level, then valve 6 is closed and helium is filled to a level of 1 bar by opening valve 1 and 3. The cleaning procedure is finished at vacuum. If hydrogen uptake is to be investigated HP is filled with hydrogen to the desired pressure by opening valves 2, 3 and 4 while keeping all other valves closed. Once the desired hydrogen pressure in HP is at the desired pressure valve 2,3, and 4 are closed and the piping is vented through valve 7 and then evacuated. The hydrogenation experiment is started by first opening valves 8, 10 and 11 (for pressure control mode) or valve valves 9 and 11 (without pressure control). All other valves are closed. Hydrogen is introduced to the sample by opening valve 4. Initially the pressure in HP will decrease rapidly due to the filling of the reactor and piping. This will be followed by an additional decrease in pressure in HP due to hydrogen uptake in the sample. If the volumes of the involved parts of the system is know the hydrogen uptake can be determined directly from the pressure drop on HP.

4.3.2 Dehydrogenation

Once hydrogenated the dehydrogenation of the sample is initiated by closing valve 4 and opening valve 5 to LP (which is at vacuum level). Initially the pressure is equalized resulting in a rapid pressure increase in LP followed by an additional increase due to hydrogen desorption from the sample in the reactor. During dehydrogenation the PC should be bypassed by keeping valves 8 and 10 closed and valve 9 open. If the volumes of the involved parts of the system is know the hydrogen desorption can be determined directly from the pressure rise in LP.

4.4 Principle of calculating hydrogen uptake

During calculations we will use the symbols defined in the table 2

Symbol	Unit	Description
T_I	K	Inlet gas reservoir temperature
T_R	K	Reactor temperature
T_D	K	Dead volume (piping) temperature
V_I	m^3	Inlet gas reservoir volume
V_R	m^3	Reactor volume
V_D	m^3	Dead volume (piping)
P_I	Pa	Inlet gas reservoir pressure
P_R	Pa	Reactor pressure
P_D	Pa	Dead volume (piping) pressure

Table 2: Symbols used in the calculation of the hydrogen uptake

Figure 10 shows which part of the experimental setup the symbols refer to.

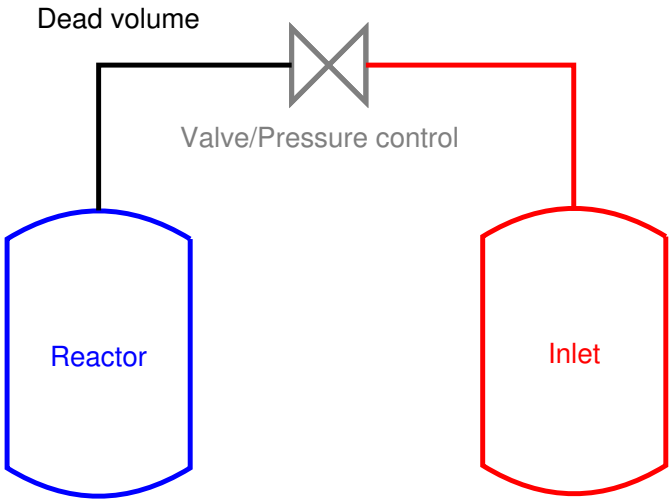

Figure 10: Definitions of the different parts of the setup. Reactor: blue, Inlet: red and Dead volume: black.

We make the following assumptions:

- $P_R = P_D$, thus we skip the symbol P_D and use only P_R to denote the pressure on the reactor side of the setup.
- $T_I = T_D$ thus we skip the symbol T_I and use only T_R to denote the temperature in both the inlet and dead volume, respectively. This may be a more crude assumption, since some heat transfer from the reactor to piping connected to it, must be expected.
- T_I is assumed constant as a function of time and equal to room temperature.
- V_I, V_R and V_D are all assumed constant.

Since some parameters/variables change with time the following sub-scripts are used to distinguish between parameters at different times (we use P_I as an example but the sub-scripts may be applied to all variables)

Symbol	Description
$P_{I,0}$	Initial state i.e. at t=0
$P_{I,f}$	Final state i.e. when the experiment is done
$P_I(t)$	Variable at time t

Table 3: Sub-scripts used in the calculation of the hydrogen uptake

Since we use pressure changes in order to calculate the hydrogen uptake it is convenient to define the following variables: $\Delta P_I = P_{I,f} - P_{I,0}$, $\Delta P_I(t) = P_I(t) - P_{I,0}$, $\Delta P_R = P_{R,f} - P_{R,0}$ and $\Delta P_R(t) = P_R(t) - P_{I,0}$.

Figure 11 shows the evolution in pressure in the inlet side and the reactor side of the system during a generic hydrogenation run in pressure control mode viz. with valve 9 closed and valves 8 and 10 open.

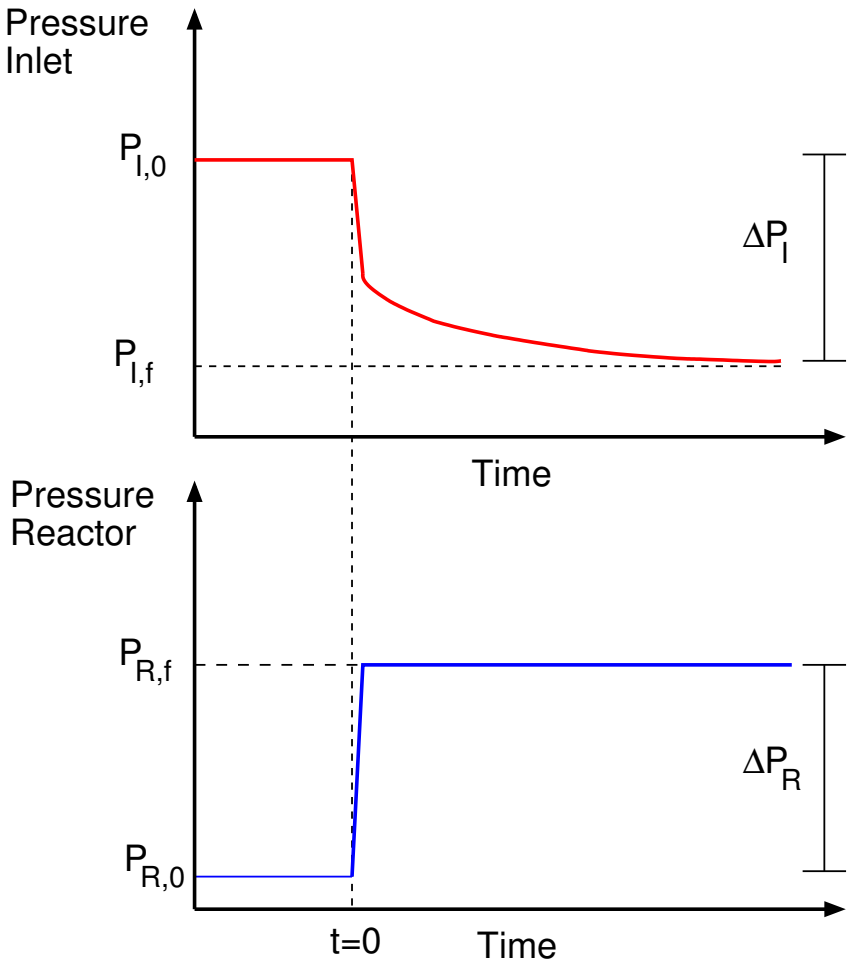

Figure 11: Pressure evolution in the inlet side and the reactor side as a function of time for a generic hydrogenation run. Reactor: blue, Inlet: red.

Before a hydrogenation run is started (t=0) the pressure in the inlet side and in the reactor side is $P_{I,0}$ and $P_{R,0}$, respectively, and $P_{I,0} > P_{R,0}$ (in most cases $P_{R,0}$ will be at vacuum level). The hydrogenation is started by opening a valve (handled by the pressure controller) between the inlet and the reactor. This causes the pressure in the inlet to drop rapidly due to the filling of the reactor to the desired level ($P_{R,f}$). Subsequently the pressure in the inlet will drop further due to the hydrogen uptake in the reactor and reach $P_{I,f}$[5]. If the volumes of the different parts of the system is known sufficiently accurately we can now calculate the hydrogen uptake.

The total loss of hydrogen in the inlet can be calculated with the *ideal gas law*:

$$\Delta n_{tot} = \frac{\Delta P_I V_I}{RT_I} \tag{6}$$

The amount required to fill the reactor to $P_{R,f}$ is given by:

$$\Delta n_{fill} = \frac{\Delta P_R V_R}{RT_R} + \frac{\Delta P_R V_D}{RT_D} \tag{7}$$

Thus, the hydrogen uptake can be found by subtraction of the two:

$$n_{uptake} = \Delta n_{tot} - \Delta n_{fill} \tag{8}$$

We may use this to express the uptake in wt. %

$$uptake\ wt.\% = \frac{n_{uptake} M_{H_2}}{m_{sample} + n_{uptake} M_{H_2}} \tag{9}$$

ΔP_I and ΔP_R in equations 6 and 7, respectively, can be substituted with their time dependent counterparts in order to calculate the hydrogen uptake *on-line*.

If hydrogenation is performed in non-pressure control mode viz. with valves 8 and 10 closed and valve 9 open instead $P_R(t) = P_I(t)$. The initial amount of hydrogen is

$$n_{start} = \frac{\Delta P_{I,0} V_I}{RT_I} \tag{10}$$

The total amount of hydrogen at time t is given by:

$$n_{tot}(t) = P_I(t) \left(\frac{(V_I + V_D)}{RT_I} + \frac{V_R}{RT_R} \right) \tag{11}$$

The uptake of hydrogen can be found from the difference

$$\Delta n_{uptake}(t) = n_{start} - n_{tot}(t) \tag{12}$$

The calculation of the released amount of hydrogen during dehydrogenation is analogous to the example above with the difference that $P_{I,0} < P_{R,0}$ and $P_{I,f} > P_{I,0}$ i.e. the net flow of hydrogen is from the reactor to the inlet[6].

[5] $P_{I,f}$ should exceed $P_{R,f}$

[6] The inlet container is actually different at dehydrogenation to that at hydrogenation (larger volume).

4.5 Determination of equipment volumes

In order to accurately calculate hydrogen uptake and desorption knowledge of the different volumes in the setup is needed. In order to determine the volumes the HP vessel is used as a reference. The HP cylinder volume have been determined by filling with liquid water and was found to be 326.8 cm^3. Further we estimate the volume of the piping between HP, valve 4 and the pressure transducer to be 2 cm^3 and probably lower. The estimated maximum error introduced on other determined volumes by this assumption is estimated to be 2/326.8·100= 0.6%. The volume of the other parts of the system is found by filling helium in HP and pumping down all other parts to vacuum level (10^{-2} mbar). Subsequently the gas in HP is expanded to the part of the system for which the corresponding volume is to be determined. The volume for this part of the system, denoted X, can be found directly from the observed pressure drop.

$$V_X = \frac{P_{HP,0} V_{HP}}{P_{HP,f}} - V_{HP} \tag{13}$$

The volume of different parts of the system is summarized in the following tables. The measured volumes are indicated by red color on the schematic system setups showed on top of each table.

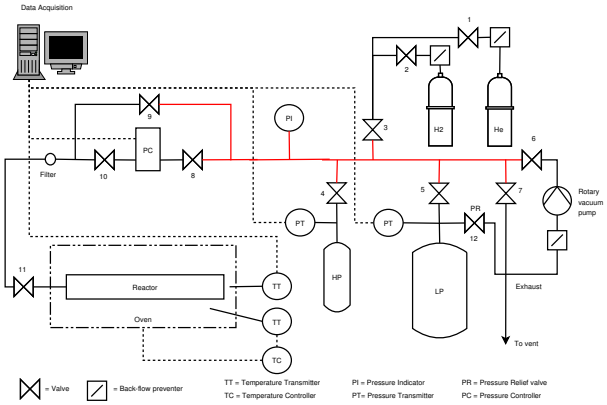

Figure 12: Indication of the measured volume in the experimental setup by expansion of gas in HP vessel. The measured volume is indicated by red color.

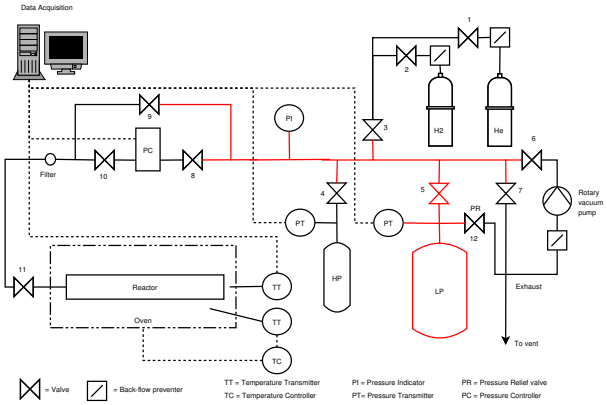

Figure 13: Indication of the measured volume in the experimental setup by expansion of gas in HP vessel. The measured volume is indicated by red color.

Measurement	Time [min]	P_i [bar]	P_f [bar]	V [cm^3]
1	1	32.47	29.90	28.26
	2	32.47	29.90	28.26
	3	32.47	29.90	28.26
	4	32.47	29.90	28.26
	5	32.47	29.90	28.26
2	2	29.91	27.54	28.30
3	2	27.56	25.38	28.24
4	2	25.39	23.39	28.12
Mean				28.23
St.Dev.				0.08

Table 4: Measurements of the pressure drop in HP vessel when expanded to piping and the corresponding volume.

Measurement	Time [min]	P_i [bar]	P_f [bar]	V [cm^3]
1	5	31.71	2.03	4790.16
2	5	29.62	1.90	4797.02
3	5	28.85	1.85	4798.70
4	5	27.98	1.79	4810.77
Mean				4799.16
St.Dev.				8.57

Table 5: Measurements of the pressure drop in HP vessel when expanded to LP vessel and the corresponding volume.

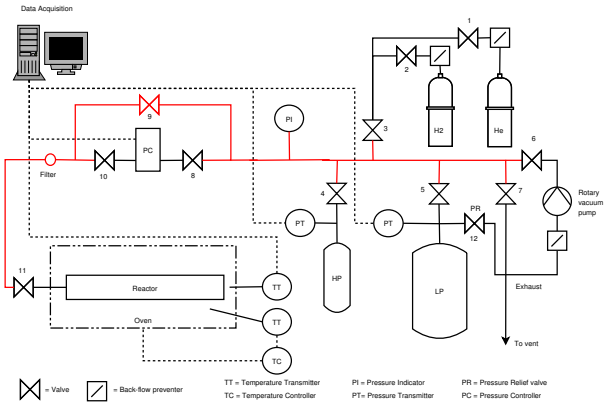

Figure 14: Indication of the measured volume in the experimental setup by expansion of gas in HP vessel. The measured volume is indicated by red color.

Measurement	Time [min]	P_i [bar]	P_f [bar]	V [cm^3]
1	2	27.17	23.47	51.83
2	2	23.48	20.34	50.76
3	2	20.35	17.63	50.73
4	2	17.64	15.30	50.29
Mean				50.90
St.Dev.				0.66

Table 6: Measurements of the pressure drop in HP vessel when expanded to piping and the corresponding volume.

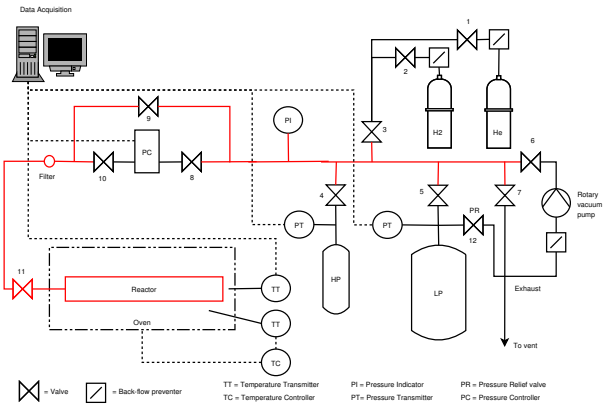

Figure 15: Indication of the measured volume in the experimental setup by expansion of gas in HP vessel. The measured volume is indicated by red color.

Measurement	Time [min]	P_i [bar]	P_f [bar]	V [cm^3]
1	2	26.78	22.44	63.59
2	2	23.27	19.57	62.16
3	2	26.50	22.26	62.63
4	2	22.27	18.72	62.35
Mean				62.68
St.Dev.				0.63

Table 7: Measurements of the pressure drop in HP vessel when expanded to piping and reactor and the corresponding volume.

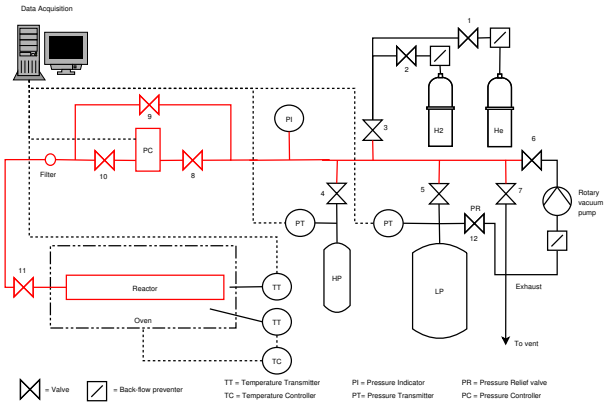

Figure 16: Indication of the measured volume in the experimental setup by expansion of gas in HP vessel. The measured volume is indicated by red color.

Measurement	Time [min]	P_i [bar]	P_f [bar]	V [cm^3]
1	2	18.73	14.87	85.35
2	2	14.89	11.84	84..70
3	2	26.00	20.62	85.79
4	2	20.62	16.37	85.36
Mean				85.23
St.Dev.				0.46

Table 8: Measurements of the pressure drop in HP vessel when expanded to piping,reactor, and pressure control and the corresponding volume.

5 Technical specifications

5.1 Valves and fittings

See table 5.1. Pictures and specifications are from the Hoke website[7].

5.2 Piping

See table 5.2.

5.3 Reactor and pressure vessels

The HP vessel is a 300 ml (according to the previous section the volume have been determined to be 326.8 ml) Hoke 304 stainless steel cylinder model 4HS300 with DOT rating 3E1800. The HP vessel is shown in figure 17. The maximum allowed pressure is reported to be 125 bar.

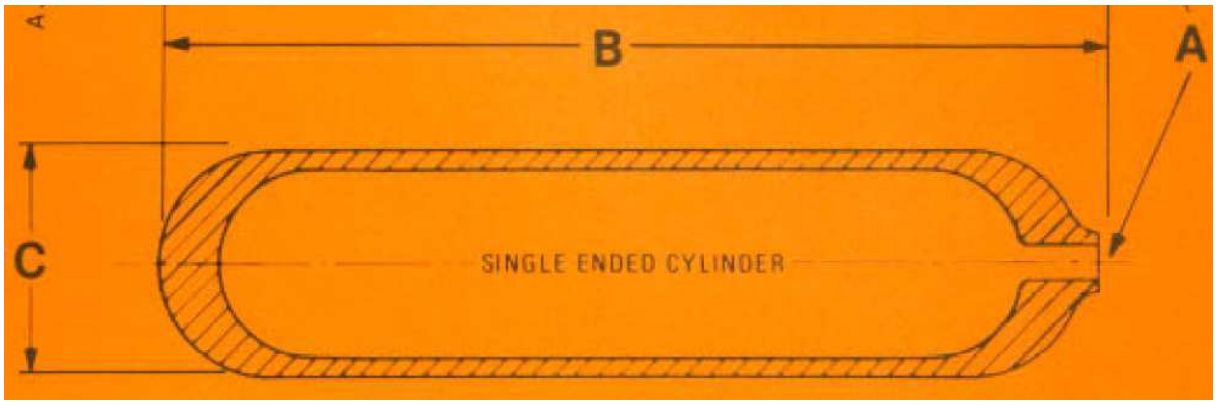

Figure 17: Hoke 4HS300 300 ml pressure cylinder used for HP vessel. The picture is from the Hoke website (see footnote 7 on page 27)

The LP pressure vessel (cf. figure 7) have previously been used for a similar purpose as a part of a hydrogen cycling rig described in more detail in ref. [5, 16, 17]. The vessel is made from stainless steel. No information about the maximum pressure allowed for this vessel have been found. Using sound judgment we expect that the vessel should be able to withstand a pressure of at least 10 bar (probably even more) without bursting. For safety reasons it is only intended for use up to a maximum of 2 bar pressure. A pressure relief valve is also added which have been set to blow at approx. 3.5 bar.

The reactor is made from stainless steel and a schematic drawing is shown in figure 18. The wall thickness of the reactor is 3.5 mm outside the heating zone and 6.5 mm inside the heating zone, respectively. Taking this into account the reactor is expected to withstand a pressure of at least 100 bar even at elevated temperatures (up to 500 °C).

5.4 Pressure measurement

The setup is equipped with 2 Kistler 4043A Piezoresistive pressure transducers cf. figure 19. The technical specifications of the available transducers are summarized in table 5.4. The picture and specifications are from the Kistler website[8].

[7] http://www.hoke.com
[8] http://www.kistler.com

Technical Data			
Model	Description	P_{max} [bar]	Pic
Hoke 691F-G4Y	Back-flow prevent.	345	
Hoke 632-G4Y	XX Micron filter	345	
Hoke 1315-G4Y	Needle valve	345	
Hoke 3752-G4Y	Needle valve	345	
Hoke 7188G4Y	Ball valve	138	
Hoke 4LU	Elbow fitting	see note	
Hoke 4TTT	Tee fitting	see note	
Hoke 4P	Plug	see note	
Note: According to the vendor HOKE Gyrolock fittings are rated for higher working pressures than the tubing recommended for use HOKE Gyrolock.			

Table 9: Summary of the valves and fittings used. All equipment is in Stainless steel (316) and 1/4” sizing.

Technical data	Wall thickness [mm]					
	0.4	0.5	0.7	0.9	1.2	1.6
Max. working pres. [bar]	153	193	279	356	521	710
Calculated burst pres. [bar]	612	772	1116	1424	2084	2840

Table 10: Maximum allowed working pressure and calculated burst pressure for 1/4” stainless steel (316) tubing according to the Hoke website (see footnote 7 on page 27).

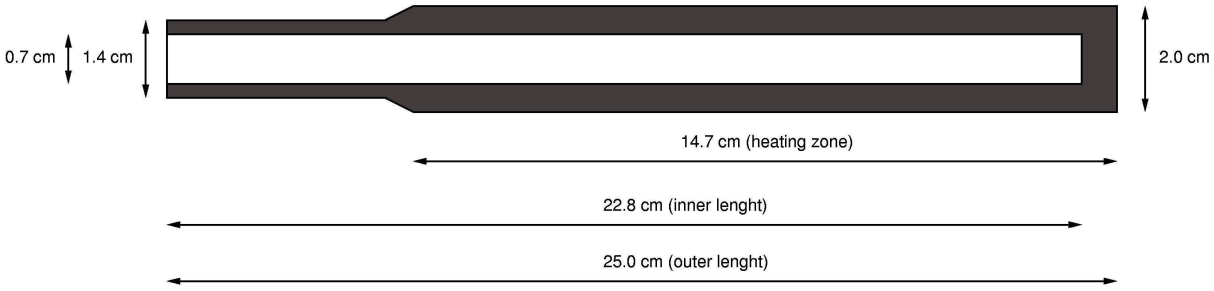

Figure 18: Drawing of the reactor part of the setup.

Technical Data		Kistler 4043A		
		A2	A50	A1000
Temperature range	°C		-20 . . . 50	
Pressure range	bar(abs)	0-2	0-50	0-100
Overload	bar(abs)	5	125	250
Linearity	%FSO	$\leq \pm 0.3$	$\leq \pm 0.3$	$\leq \pm 0.3$
Sensitivity	mV/bar	250	10	5
Natural frequency	kHz	> 20	> 110	> 150
Tightening torque	Nm		12. . . 20	
Weight	g		3	
Connector			Fischer type SE 102A054	
Full range signal	mV		500	
Calibration current	mA		2. . . 5	
Input/output impedance	kΩ		$\approx$3	
Stability of sensitivity	%/a		$<$0.2	
Stability of zero measured output	%FSO		$<$0.5	
Thermal zero shift	%FSO		$\leq \pm 0.5$	
Thermal sensitivity shift	%		$\leq \pm 1$	
Acceleration error	bar/g		$< 3 \cdot 10^{-4}$	
Shock resistance	g		1000	
Volume change	mm^3		$<$0.2	

Table 11: Technical specifications for Kistler 4043A Piezoresistive pressure transducers

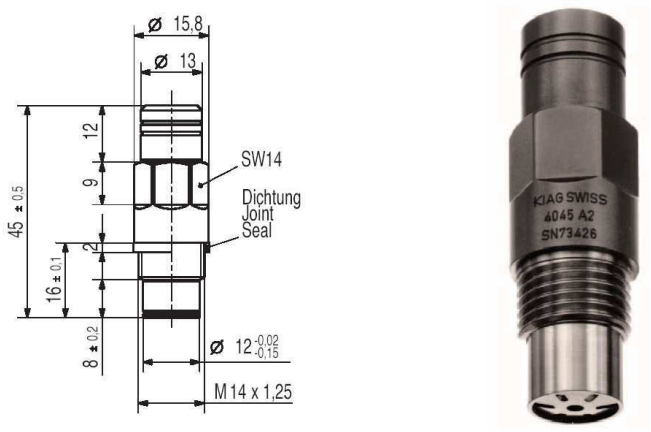

Figure 19: Kistler Piezoresistive Absolute Pressure Sensor 4043A

The 0-500 mV signal from the pressure transducers are amplified to 0-1 V (0-10 V optional) by two Kistler/KIAG 4601 piezoresistive amplifiers. The amplifiers were purchased by Risø in the early eighties and no documentation exist but the amplifiers are probably comparable in specification with the newer 4603B (specifications can be found at the Kistler website).

5.5 Pressure control

The pressure controller used in the experimental setup is shown in figure 20 and the technical specifications are summarized in table 5.5. The operation mode of the controller is shown in figure 21 and is set to *downstream control* i.e. the pressure controller measures the pressure in the vessel downstream (PV) and acts in such manner that the downstream pressure is kept at the desired value (SP). The pictures and specifications are from the Brooks Instruments website[9]. The pressure controller is powered by a Skytronic 650.685 laboratory power supply[10].

[9] `http://www.brooksinstruments.com`

[10] See the Skytronics website for additional information `http://www.skytronic.com`.

Figure 20: The Brooks 5866E pressure controller

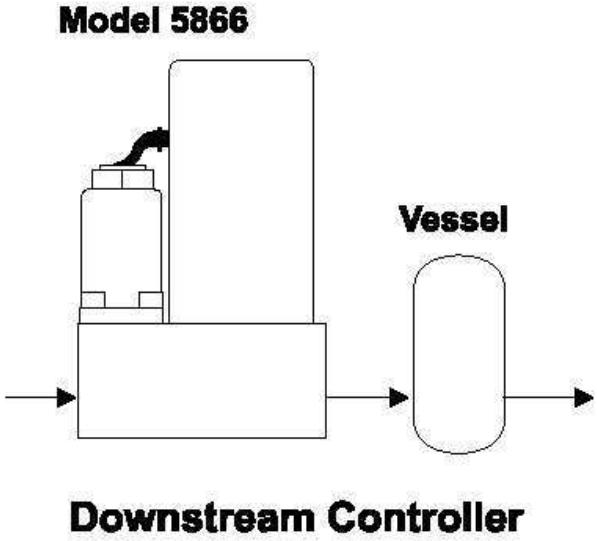

Figure 21: The Brooks 5866E pressure controller regulation mode

Technical Data		Brooks 5866E
Pressure range	bar	7.25 psia to 1450 psia full scale
Flow range	cm^3	0...30000
Control range		20 to 1
Accuracy	%FS	$\pm$ 0.5
Repeatability	%FS	$\pm$0.1
Max. pressure	bar	300
Max. transducer	bar	435 psia for 72.5-290 psia full scale
Leak integrity, Inboard to outboard		1 x 10 -9 atm cc/sec Helium max.
Temperature coefficient	%FS/$^\circ$C	0.1
Zero stability	%FS/30days	0.001
Input/output offset	%FS (voltage)	$<$0.2
Proportional gain		1...200
Integration time	s	0.05...5
Electrical connections		D-type connector (DA-15P)
Remote pre. sensor input	Vdc	0-10
Pressure set point signal	Vdc	0-5(optional 0-10)
Power requirement(N.C.)		3.5 watts; +15 Vdc ($\pm$5%) at 30 mA
		-15 Vdc ($\pm$5%) at 170 mA

Table 12: Technical specifications for Brooks 5866E pressure controller

5.6 Vacuum system

The experimental setup is equipped with a Leybold TRIVAC D16B rotary vacuum pump. A zeolite trap is mounted upstream in order to prevent oil vapor back diffusion from the pump to the system. The technical specifications of the vacuum pump is summarized in table 5.6 and pumping characteristics are shown in figures 22-23. The pictures and specifications are from the Leybold website[11].

Technical Data		TRIVAC D 16 B	
		50 Hz	60 Hz
Nominal pumping speed[1]	m^3h^{-1}	18.9	22.7
Pumping speed[1]	m^3h^{-1}	16.5	19.8
Ultimate partial pressure without gas ballast[1]	mbar	10^{-4}	
Ultimate total pressure without gas ballast[1]	mbar	$<$2 x 10^{-3}	
Ultimate total pressure with gas ballast[1]	mbar	< 5 x 10^{-3}	
Water vapor tolerance[1]	mbar	25	
Water vapor capacity	gm/h	305	
Oil filling, min./max.	l	0.5 / 1.0 (0.5 / 1.1)	
Noise level* to DIN 45 635, without/with gas ballast	dB(A)	52 / 54	
Admissible ambient temperature	°C	12 - 40	
Motor rating*	W (HP)	750 (1)	
Nominal speed	rpm	1500	1800
Type of protection	IP	54	
Weight*	kg	26	
Connections, Intake and Exhaust	DN	25 KF	

[1] To DIN 28 400 and following numbers

* Weight, motor rating and noise levels
for the pumps with 230 V, 50 Hz AC motor only.

Table 13: Technical specifications for Leybold TRIVAC D16B rotary vane vacuum pump

5.7 Temperature control and measurement

The reactor is heated by a Carbolite MTF 12/25/250 tube furnace (cf. fig. 8). The heating zone of the oven is 250 mm long with a diameter of 25 mm. The heating power is 0.7 kW. The temperature is controlled and displayed by a Carbolite type 210 temperature (made by Eurotherm) controller. The temperature controller operates with a PID (Proportional, Integral and Differential) control algorithm (see ref. [18] for further information about control algorithms). The maximum temperature accessible with the oven is 1200 °C. To improve temperature uniformity in the heating zone and thus in the reactor an alumina plug is inserted in one end of the furnace tube. The reactor temperature (actually the oven temperature) is measured with a Ni-Cr/Ni thermocouple (type K) inserted through the alumina plug.

[11] http://www.leyboldvac.de/product/trivac/index.htm

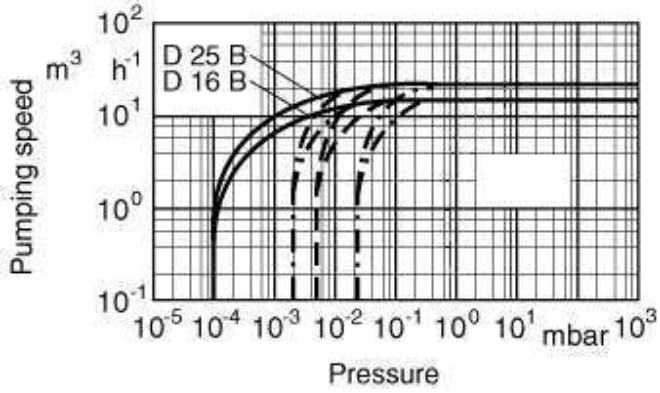

Figure 22: Pumping speed characteristics of Leybold TRIVAC D16B rotary vane vacuum pump

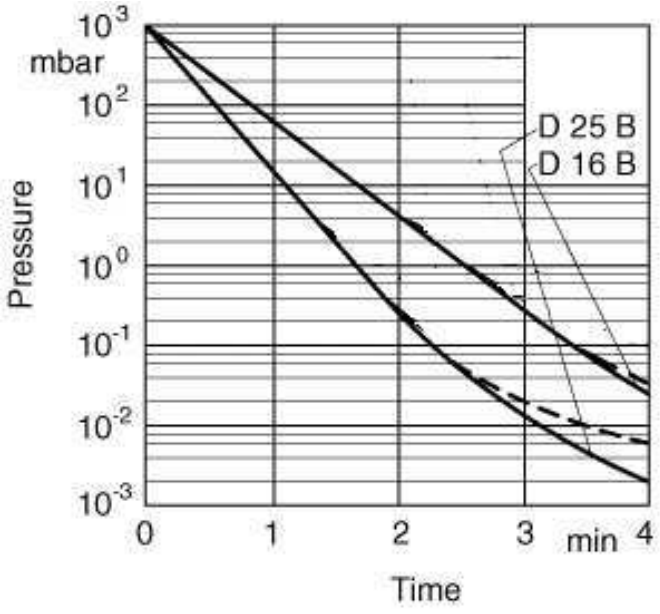

Figure 23: Pump-down characteristics of a 100 l vessel using a Leybold TRIVAC D16B rotary vane vacuum pump

5.8 Data acquisition hardware

Data acquisition (DAQ) from Kistler pressure sensors, oven thermocouple, and pressure sensor in the Brooks pressure controller is handled by a National Instruments PCI-6040E (formerly known as PCI-MIO-16E-4) DAQ card with 16 analog input multifunction channels and 2 analog output channels. The sample rate is 250 kS/s (multichannel) with a resolution of 12-Bit. The output of the piezoresistive amplifiers and the amplified signal from the thermocouple is connected to the card via a National Instruments SCB-68 68 pin shielded connector block[12].

[12] See the National Instruments website for additional information about the DAQ device and connector block: `http://www.ni.com`.

6 Software

6.1 LabView data acquisition

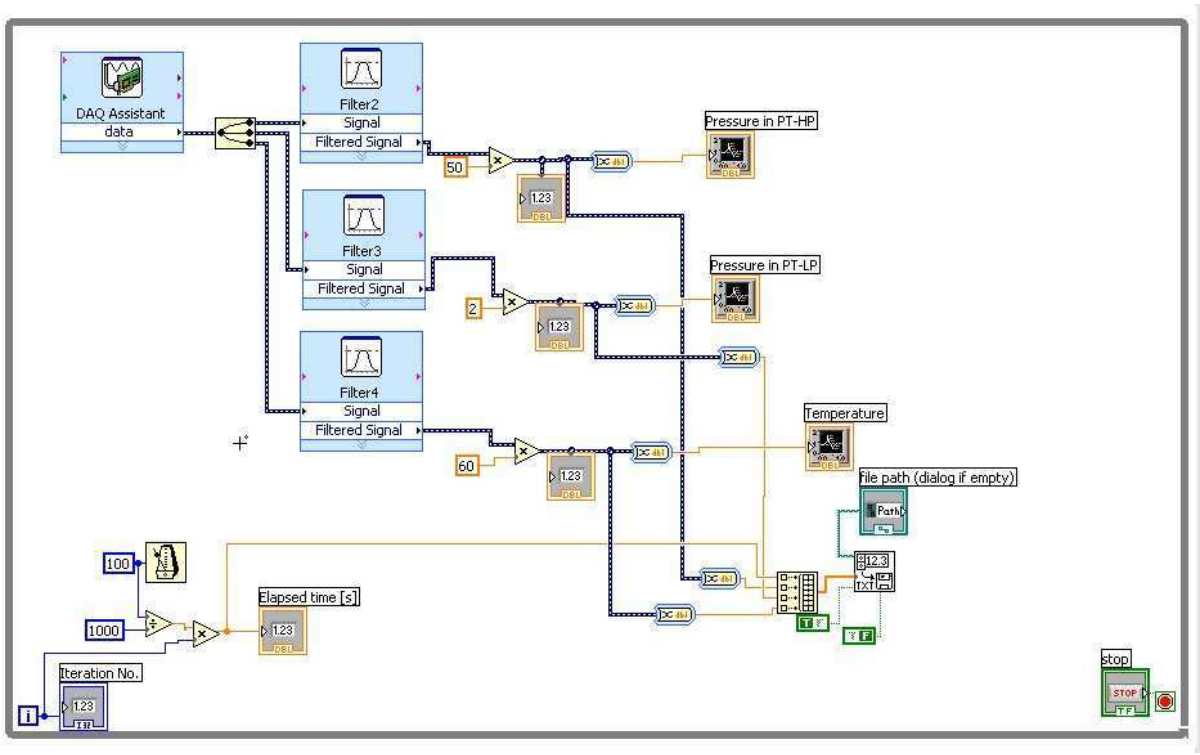

Figure 24: Screen shot of the LabView block diagram for data acquisition, conditioning and storage.

National Instruments LabView 7.0 have been chosen as a platform for data handling including acquisition, conditioning and storage. Figure 24 shows the LabView block diagram of the LabView program that have been developed for data acquisition[13]. The main features of the block diagram is readout from channels 0,1, and 2 of the NI DAQ card which represent pressure in HP, pressure in LP and oven temperature, respectively. The raw signals are filtered to reduce noise and scaled by multiplication by appropriate factors to convert from voltage to measured units viz. pressure in bar and temperature in °C. The converted data is stored in an ascii-file with the following format

```
0.000    40.583  0.000    42.934
0.100    40.582  0.000    42.927
0.200    40.580  0.000    42.920
0.300    40.579  0.000    42.934
0.400    40.578  0.000    42.920
*****    ******  *****    ******
```

where the first column is time in seconds (relative to acquisition start time), second column is pressure in HP in bar, third column is pressure in LP in bar and fourth column is oven temperature in °C. Data is acquired and stored iteratively every 0.1 sec. until the program

[13]In writing, no functionality have been applied for integration of the input(pressure measurement)/output(set point) of the pressure controller. This work is in progress.

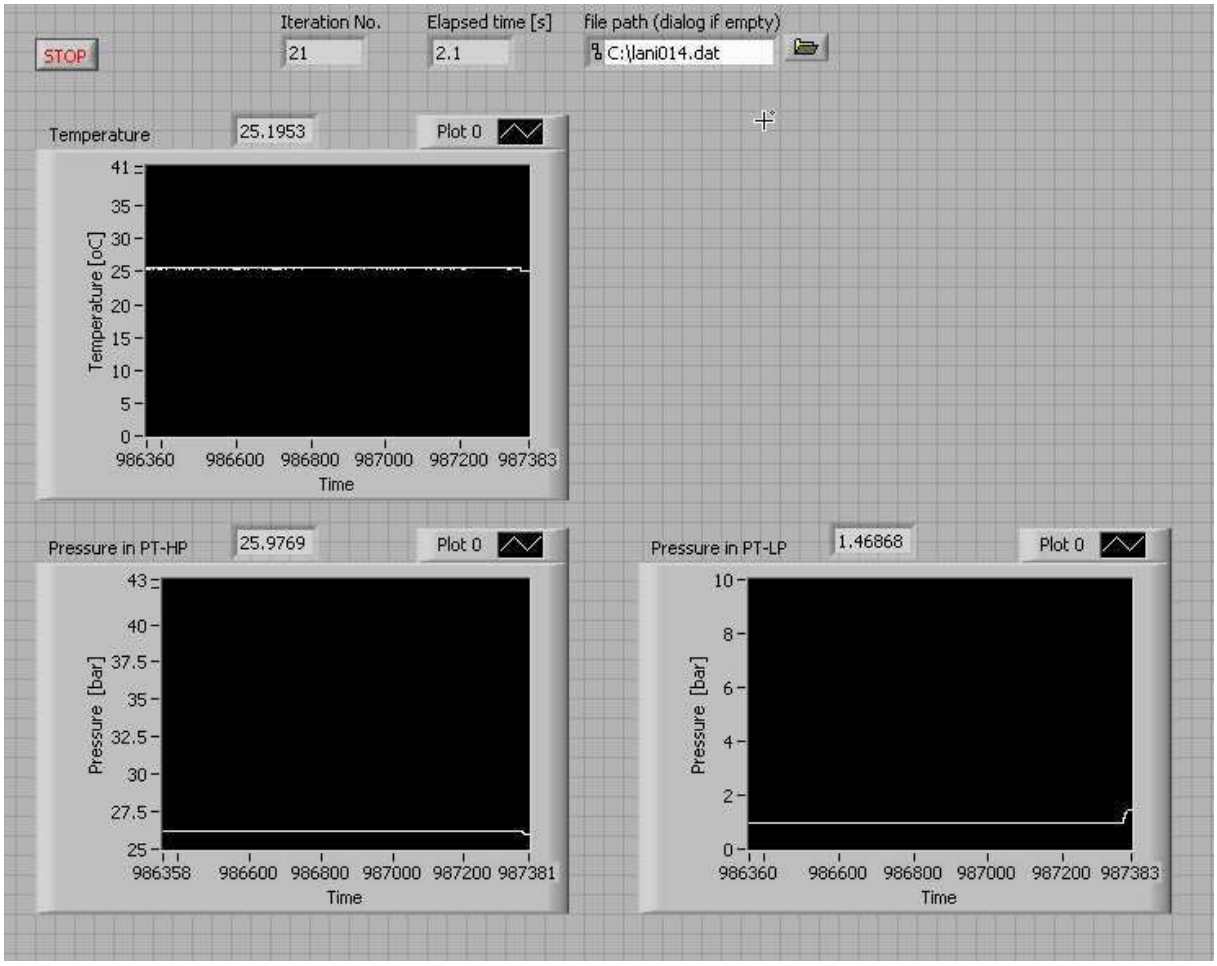

Figure 25: Screen shot of the LabView front panel (user interface) for data acquisition, conditioning and storage.

is terminated. The iteration time can be adjusted to fit the experimental conditions e.g. fast kinetics requires a small iteration time (many samplings) and for slow kinetics a longer iteration time (fewer samplings).

Figure 25 shows the user interface of the LabView program. The user interface allows specification of file name for data storage, start/stop of data acquisition, display of measured pressures and temperatures both numerically and graphically. Further, the iteration number and the corresponding time are displayed numerically.

6.2 Post processing of data

In order to calculate hydrogen uptake/release two Octave scripts have been written for this purpose. The scripts are more or less self explaining.

6.2.1 `GNU/Octave` script for calculating uptake

```
clear

%-------------------------------------------------------
```

```
% Reading raw-data and assigning data vectors
%-------------------------------------------------------------
load -force lani013.dat
data = lani013;
time = data(:,1);
P_HP = data(:,2)*1e5;
P_LP = data(:,3)*1e5;
T_reac = data(:,4)+273.15;
%-------------------------------------------------------------
% System constants
%-------------------------------------------------------------
sample_mass=20.73;
sample_molarmass=432.3725;
Vol_HP=326.8e-6;
Vol_pipe=50.9e-6;
Vol_reac=7.3e-6;
Vol_LP=4799.16e-6;
T_room=26+273.15;
R=8.314;
samplepoints=length(time);
%-------------------------------------------------------------
% Calculating hydrogen uptake
%-------------------------------------------------------------
n_start=P_HP(1)*Vol_HP/(R*T_room)+ ...
P_LP(1)*Vol_pipe/(R*T_room)+...
P_LP(1)*Vol_reac/(R*T_reac(1));

n_end=P_HP(samplepoints)*(Vol_HP+Vol_pipe)/...
(R*T_room)+P_HP(samplepoints)*(Vol_reac)/...
(R*T_reac(samplepoints));
n_uptaketot=n_start-n_end;
weightpercent=n_uptaketot*2.016/...
(n_uptaketot*2.016+sample_mass)*100
HM=n_uptaketot*2.016/(6*sample_mass/sample_molarmass);
n = P_HP*(Vol_HP+Vol_pipe)/(R*T_room)+P_HP*(Vol_reac)./(R*T_reac);
n_uptake = n_start -n;
weight_uptake=n_uptake*2.016./...
(n_uptake*2.016+sample_mass)*100;
%-------------------------------------------------------------
% Finding start time
%-------------------------------------------------------------
k=1;
while weight_uptake(k)< 0
start_time=time(k);
k=k+1;
end
time=time-start_time;
%-------------------------------------------------------------
% Plotting data with new start time
%-------------------------------------------------------------
```

```
figure(1)
plot(time(k:length(time)),weight_uptake(k:length(time)))
figure(2)
plot(time(k:length(time)),T_reac(k:length(time)))
figure(3)
plot(time(k:length(time)),P_HP(k:length(time)))
%-------------------------------------------------------------
% Saving data
%-------------------------------------------------------------
uptake_matrix=[time(k:length(time)) weight_uptake(k:length(time))];
temp_matrix=[time(k:length(time)),T_reac(k:length(time))];
pres_matrix=[time(k:length(time)),P_HP(k:length(time))];

save -ascii uptake.dat uptake_matrix
save -ascii pressure.dat pres_matrix
save -ascii temperature.dat temp_matrix
%-------------------------------------------------------------
% End of file
%-------------------------------------------------------------
```

6.2.2 GNU/Octave script for calculating release

```
clear

%-------------------------------------------------------------
% Reading raw-data and assigning data vectors
%-------------------------------------------------------------
load -force lani014.dat
data=lani014;
time = data(:,1);
P_HP = data(:,2)*1e5;
P_LP = data(:,3)*1e5;
T_reac = data(:,4)+273.15;
%-------------------------------------------------------------
% System constants
%-------------------------------------------------------------
sample_mass=20.73;
sample_molarmass=432.3725;
Vol_HP=326.8e-6;
Vol_pipe=50.9e-6;
Vol_reac=7.3e-6;
Vol_LP=4799.16e-6;
T_room=27+273.15;
R=8.314;
samplepoints=length(time);
%-------------------------------------------------------------
% Calculating hydrogen uptake
%-------------------------------------------------------------
n_start=P_HP(1)*Vol_pipe/(R*T_room)...
+P_HP(1)*Vol_reac/(R*T_reac(1))...
```

```
+P_LP(1)*Vol_LP/(R*T_room);
n_end=P_LP(samplepoints)*(Vol_LP+Vol_pipe)/...
(R*T_room)+P_LP(samplepoints)*(Vol_reac)/...
(R*T_reac(samplepoints));
n_uptaketot=-n_start+n_end;
weightpercent=n_uptaketot*2.016/...
(n_uptaketot*2.016+sample_mass)*100
HM=n_uptaketot*2.016/(6*sample_mass/sample_molarmass);
n = P_LP*(Vol_LP+Vol_pipe)/(R*T_room)+P_LP*(Vol_reac)./(R*T_reac);
n_uptake = -n_start +n;
weight_uptake=n_uptake*2.016./...
(n_uptake*2.016+sample_mass)*100;
%-------------------------------------------------------------
% Finding start time
%-------------------------------------------------------------
k=1;
while weight_uptake(k)< 0
start_time=time(k);
k=k+1;
end
time=time-start_time;
%-------------------------------------------------------------
% Plotting data with new start time
%-------------------------------------------------------------
figure(1)
plot(time(k:length(time)),weight_uptake(k:length(time)))
figure(2)
plot(time(k:length(time)),T_reac(k:length(time)))
figure(3)
plot(time(k:length(time)),P_LP(k:length(time)))
%-------------------------------------------------------------
% Saving data
%-------------------------------------------------------------
release_matrix=[time(k:length(time)) weight_uptake(k:length(time))];
temp_matrix=[time(k:length(time)),T_reac(k:length(time))];
pres_matrix=[time(k:length(time)),P_LP(k:length(time))];

save -ascii release.dat release_matrix
save -ascii pressure.dat pres_matrix
save -ascii temperature.dat temp_matrix
%-------------------------------------------------------------
% End of file
%-------------------------------------------------------------
```

7 Test experiments

7.1 Leak test

Figure 26 shows the evolution in helium pressure in the setup as a function of time at room temperature. The maximum observed difference in helium pressure is 0.2 bar. This corresponds to a leak of 82 cm^3 He at ambient conditions or a leak rate of 0.05 cm^3/min. However, after approx. 18 hours the pressure starts to increase again. Considering this the observed pressure drop is probably not due to a leak, at least not exclusively, instead it might be due to temperature variations in the laboratory. The pressure change may be explained by a 1.4 °C variation in room temperature which seems plausible taking into account that the experiment has run overnight.

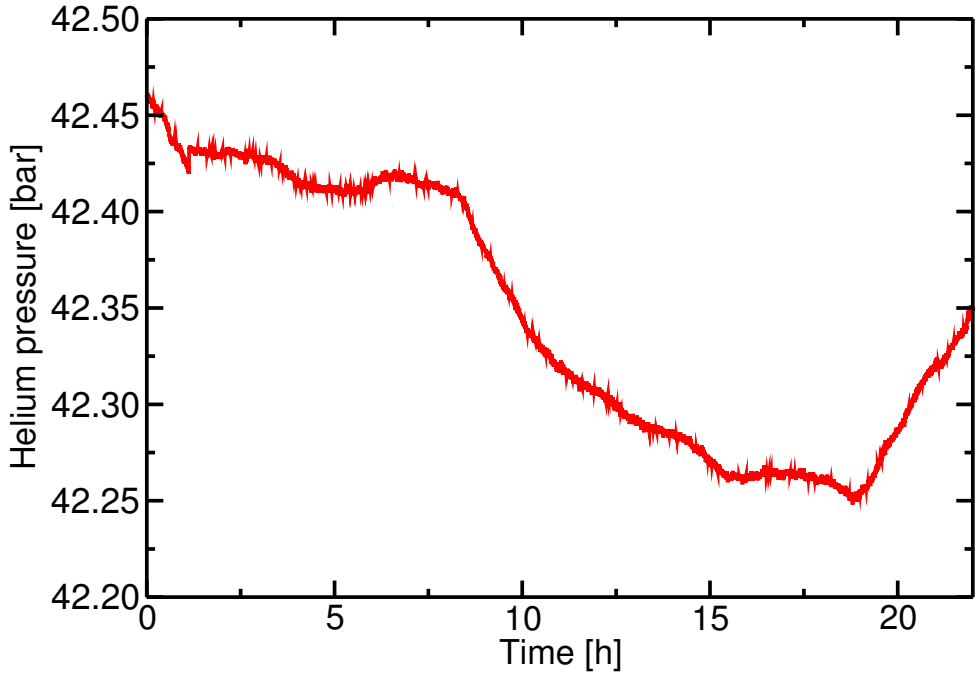

Figure 26: Helium pressure as a function of time at room temperature.

A similar experiment have been made replacing helium with hydrogen. The result is shown in figure 27. Here a maximum pressure change of 0.35 bar is observed. Near the end of the experiment the pressure seems to be increasing after it have been decreasing for almost 15 hours. Again, this indicates that the observed pressure drop may at least partially be due to something else than a leak e.g. temperature variations. Both before, during and after the experiment the complete setup was tested for leaks using a hand held TIF 8800A combustible gas detector. No detectable leaks were discovered.

The setup filled with hydrogen have also been tested for leaks with the oven and reactor heated to 400 °C. Pressure and temperature is shown as function of time in figure 28. As in the previous case no detectable leaks were found using the combustible gas detector.

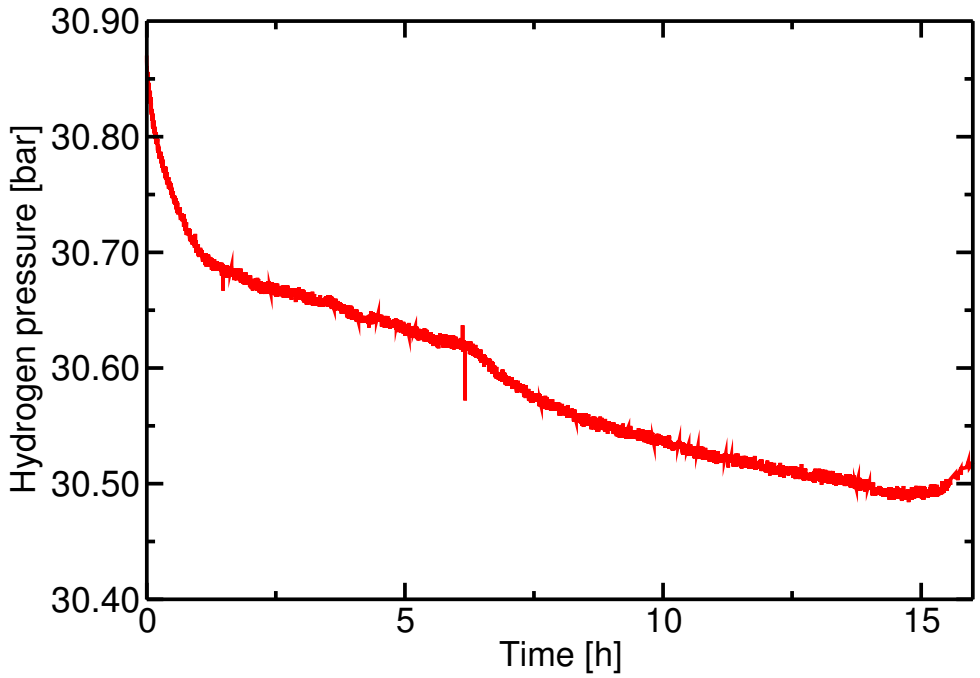

Figure 27: Hydrogen pressure as a function of time at room temperature.

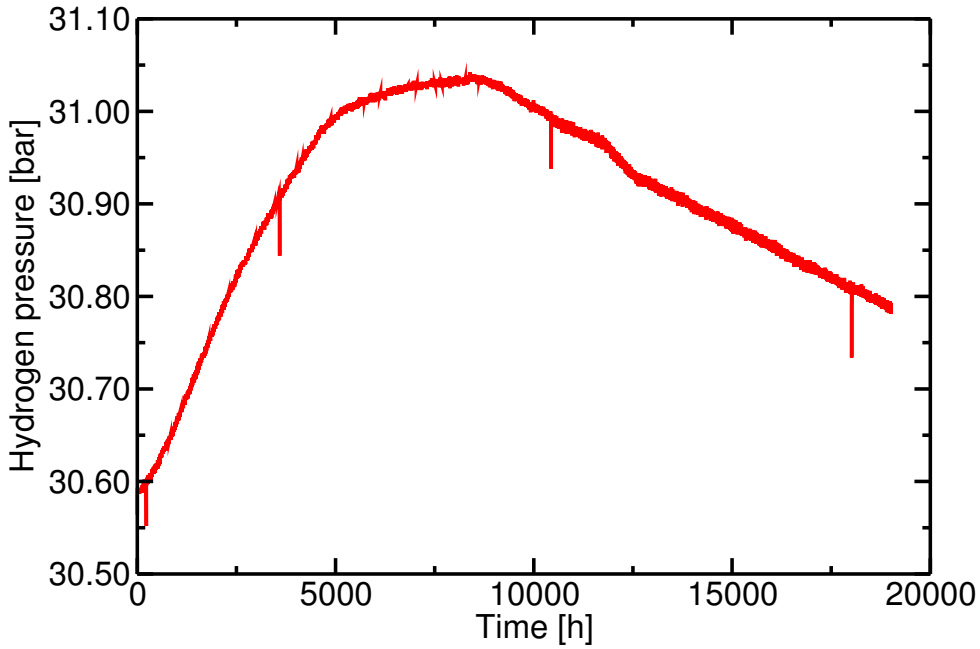

Figure 28: Hydrogen pressure and temperature as a function of time. The applied heating rate is 5 °C/min and cooling is carried out by switching of the oven reactor and turning on a fan.

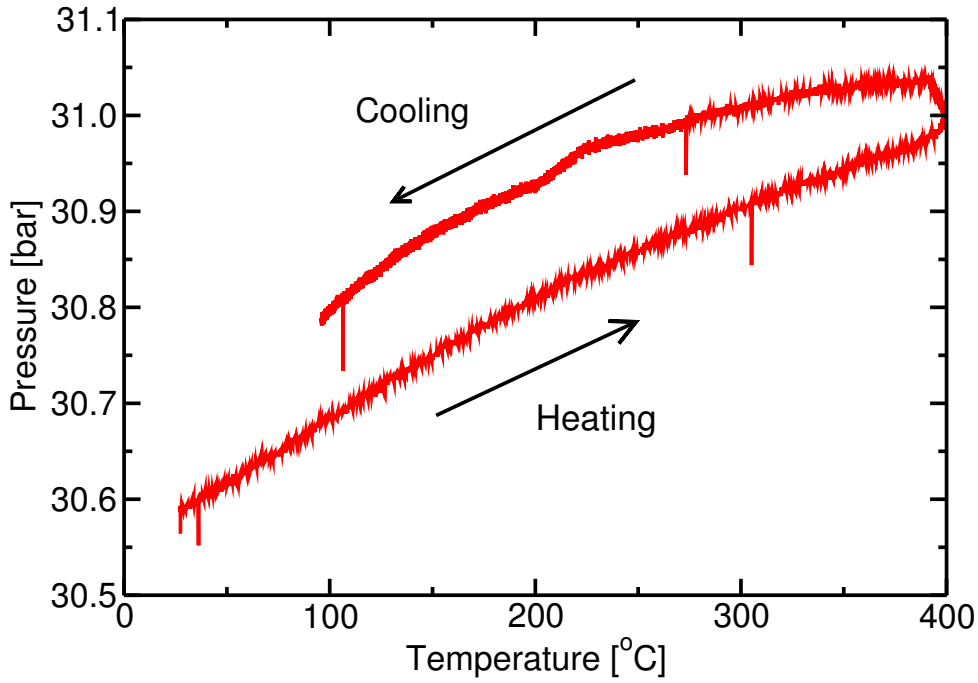

Figure 29: Hydrogen pressure as a function of temperature. The applied heating rate is 5 °C/min and cooling is carried out by switching of the oven and turning on a fan.

7.2 Oven test

The performance of the oven and the temperature control is checked by investigating corresponding temperatures and pressures both during heating (with a temperature ramp/constant heating rate) and at constant temperature regulation at elevated temperatures. Figure 28 shows temperature and pressure as a function of time during heating with a rate of 5 °C/min, at constant temperature and during cooling, respectively. As shown in the figure the pressure correlates with temperature i.e. pressure increase as a function of temperature and vice versa, as should be expected. This is also illustrated in figure 29. Some hysteresis is observed due to the fact that the pressure continues to increase even though the temperature decrease slightly at constant temperature control. This phenomenon can very well be assigned to heat transfer limitations from oven to the reactor i.e. a temperature gradient exists leading to a temperature lag between oven and reactor interior.

According to figure 28 the pressure increases from 30.59 to 31.04 bar during heating from 27 to 393 °C. Calculating the expected pressure increase using the determined volumes from section 4 (volume of reactor 12 cm^3 and volume HP and piping 399 cm^3) we get 31.09 bar assuming that the complete reactor volume is heated to 393 °C. In practice this is probably not the case since one end of the reactor sticks out of the oven end.

Although the measured temperature ramp in figure 28 looks almost linear we have investigated this in more detail by heating from RT to 80 °C and from RT to 400 °C, respectively. The results are shown in figures 30-31. The actual heating rates (the temperature controller was set to 5 °C/min) are found by taking the time derivative of the temperature signals. Both in the case of heating to 80 and 400 °C large variations in the actual heating rate are observed ranging from 0 to 10 °C/min. If the temperature signal is enlarged we find that periodic fluctuations exists. The period is found to be be approx. 2 min. with an amplitude of approx. 0.5 °C.

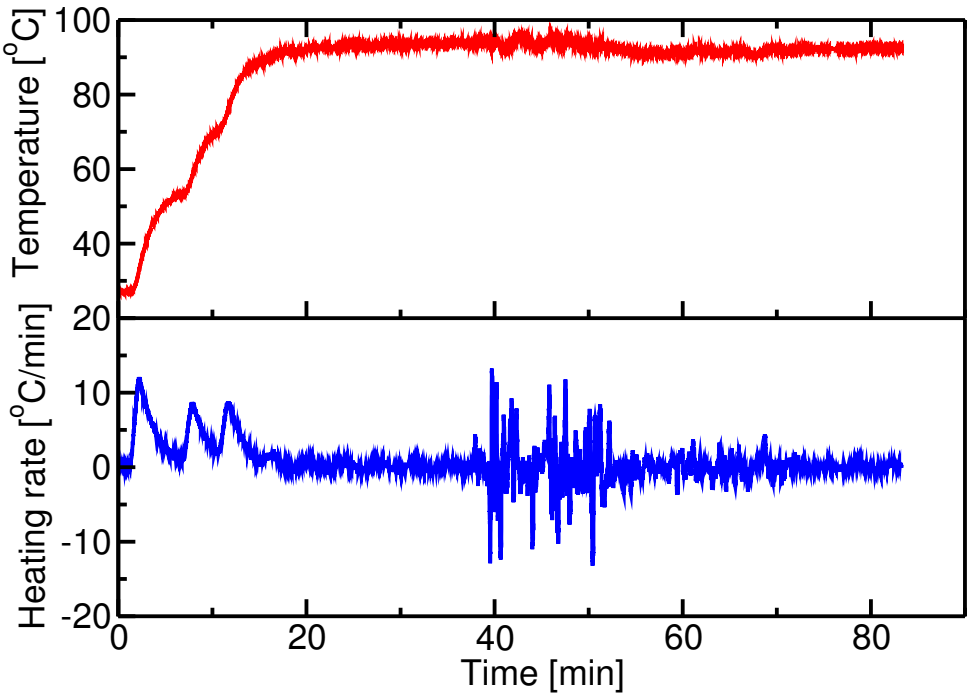

Figure 30: Temperature and heating rate as a function of time.

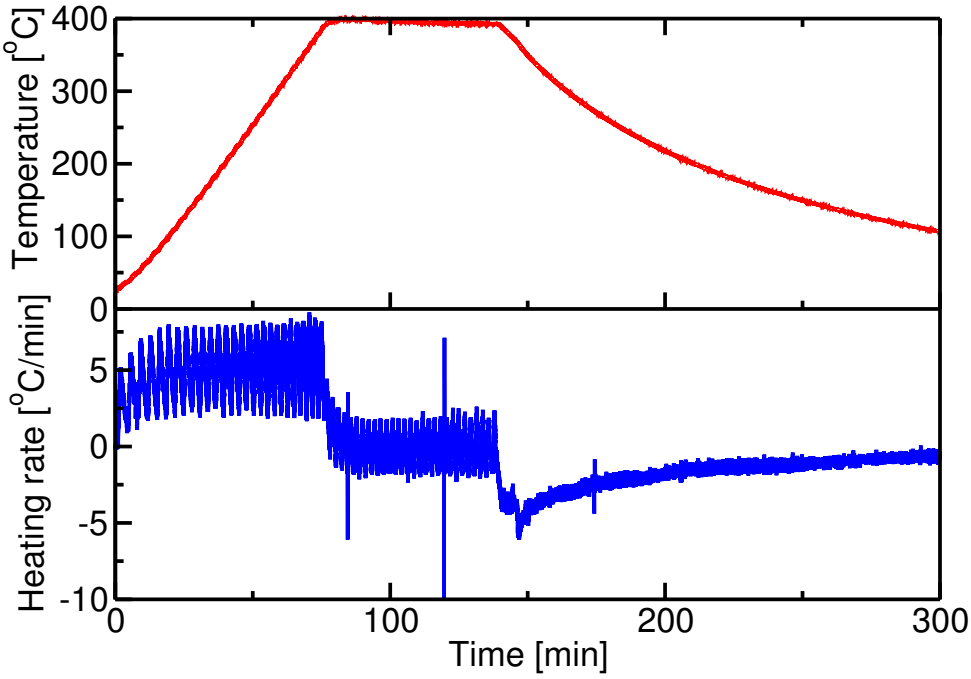

Figure 31: Temperature and heating rate as a function of time.

7.3 Hydrogen uptake in $LaNi_5$

To test the setup with respect to its ability in measuring hydrogen uptake and hydrogen desorption, respectively, we use $LaNi_5$ as a test system. The interaction of $LaNi_5$ with hydrogen is well documented in the literature and thus well suited as a test medium. $LaNi_5$ reacts fast with hydrogen forming a $LaNi_5H_6$ hydride (H/M = 1) and requires only little pretreatment (see footnote 2).

Figure 32 shows the hydrogen uptake in 20 g 99.5 % purity, -100 mesh (particle size below 150 micron) $LaNi_5$ powder from Alfa Aesar/Johnson Matthey. The uptake is found from calculations based on measured changes in pressure (and temperature) using the Octave scripts shown in the previous section. As shown in the figure the first hydrogenation is relatively slow whereas the following are significantly faster. This is a quite normal activation behaviour not only for $LaNi_5$ but for metal hydrides in general[14]. The kinetics is also improved from the 2. to the 3. cycle even despite the fact that the temperature is lowered 13 °C. According to equation 3 the rate should decrease when the temperature is lowered. However, the observation of the opposite might suggest that the sample is still not fully activated after 2. cycles. Furthermore, the overall driving force (expressed as the difference between actual pressure and the equilibrium pressure given by equation 5) increases when the temperature is reduced.

The theoretical maximum hydrogen uptake in $LaNi_5$ is 1.49 wt. % assuming a H/M ratio of 1.08 (see footnote 2). We observe a hydrogen uptake slightly above 1.35 wt. % (H/M$\approx$1) for the first two hydrogenations which seems to be in acceptable agreement with this and in agreement with the experimental observations on hydrogen uptake in $LaNi_5$ in practice [21, 22].

Ideally, the hydrogen uptake should be carried out under isothermal conditions in order to simplify data analysis. However, this setup is designed for rather large samples making this hardly realizable the heat of reaction taken into account (approx. 30 kJ/mol exothermal for $LaNi_5$). This will eventually lead to a heat up of the hydride bed in the reactor. This is illustrated for the 2. hydrogenation cycle in figure 33 showing a 5.5 °C temperature increase during reaction. In comparison with the heat of reaction (proportional to the hydrogen uptake) the temperature signal is delayed. Again this signals heat transfer limitations in the system.

Figure 34 shows hydrogen desorption for the 6 cycles measured. It is generally found that the amount of hydrogen desired is somewhat lower (approx. 1.2 wt. %) than than the amount absorbed. The reason for this behaviour may be accounted for by the the fact that absorption is initiated at vacuum level and in contrast to this desorption is finalized at approx. 1 bar of hydrogen. The difference in hydrogen absorption/desorption capacity may thus be the amount of hydrogen dissolved in $LaNi_5$ at 1 bar. According to figure 6 this is roughly 0.07 wt. % hydrogen at 49 °C. After the 3. cycle the initial pressure in the reactor is increased from vacuum level to 1 bar hydrogen and better agreement between absorption and desorption is then obtained cf. figure 35.

According to figure 34 the dehydrogenation is generally slower than hydrogenation. This can be accounted for by a higher activation energy for desorption (approx. 50 kJ/mol) than for absorption (approx. 35 kJ/mol) [23]. Besides this, the dehydrogenation proceeds somewhat unusual compared to the hydrogenation. First, no significant activation behavior is observed. This is probably because most activation was taken care of by the 1. hydrogenation. Second, no unidirectional trend in kinetics is observed e.g. 5. cycle is significantly slower than 3. cycle. One possible explanation for the apparent scatter in desorption kinetics is that since the

[14]The activation process covers different phenomena and includes penetration of the natural oxide layer on as-prepared samples (if previously exposed to air), followed by complete hydride formation, which leads to cracking of the particles, due to the expansion associated with the hydrogenation process combined with the brittle nature of most metal hydrides [19, 20]. During the first hydrogenation/dehydrogenation cycles, the reaction rate increases due to the creation of fresh contamination-free surface and/or smaller particles (higher surface area and shorter diffusion paths) until a steady-state is reached.

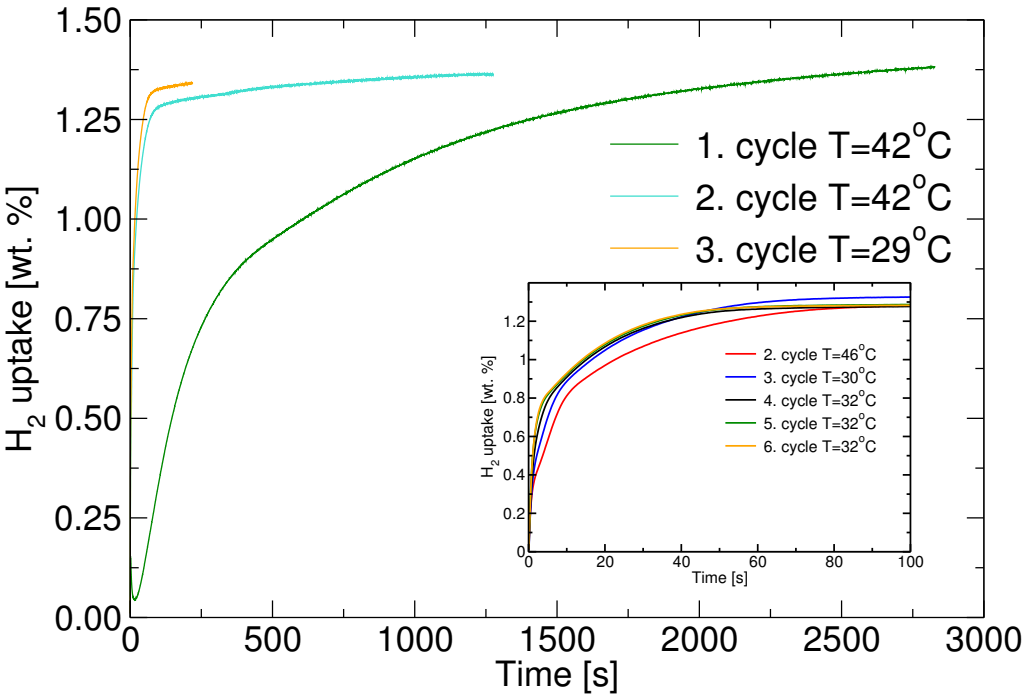

Figure 32: Hydrogen uptake in $LaNi_5$ at a hydrogen pressure in the range 25-35 bar.

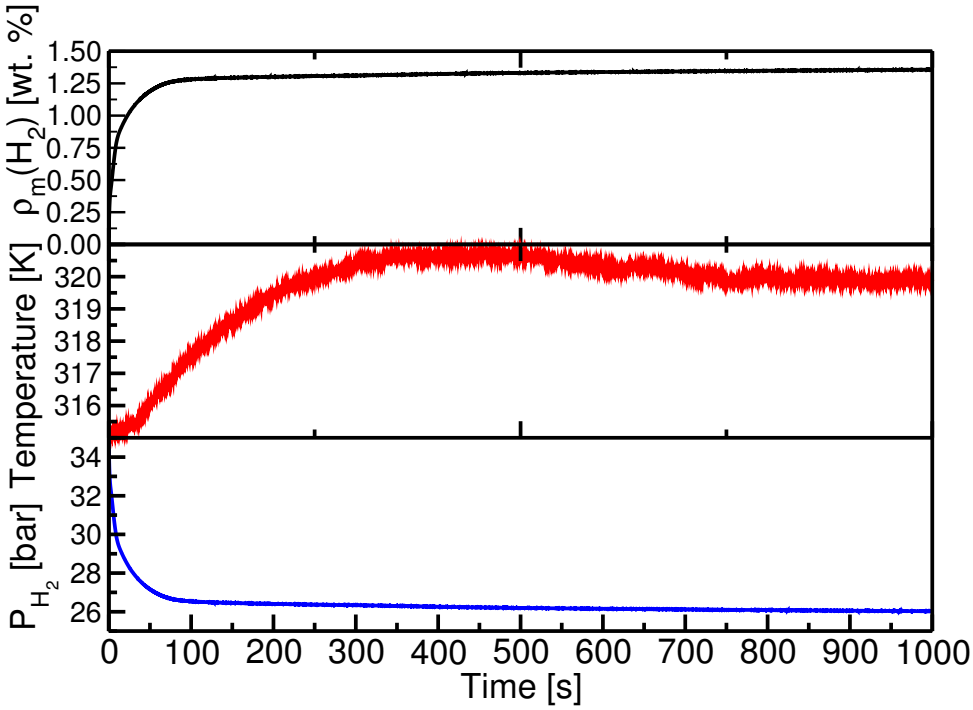

Figure 33: Hydrogen uptake, temperature and pressure for 2. cycle hydrogenation of $LaNi_5$.

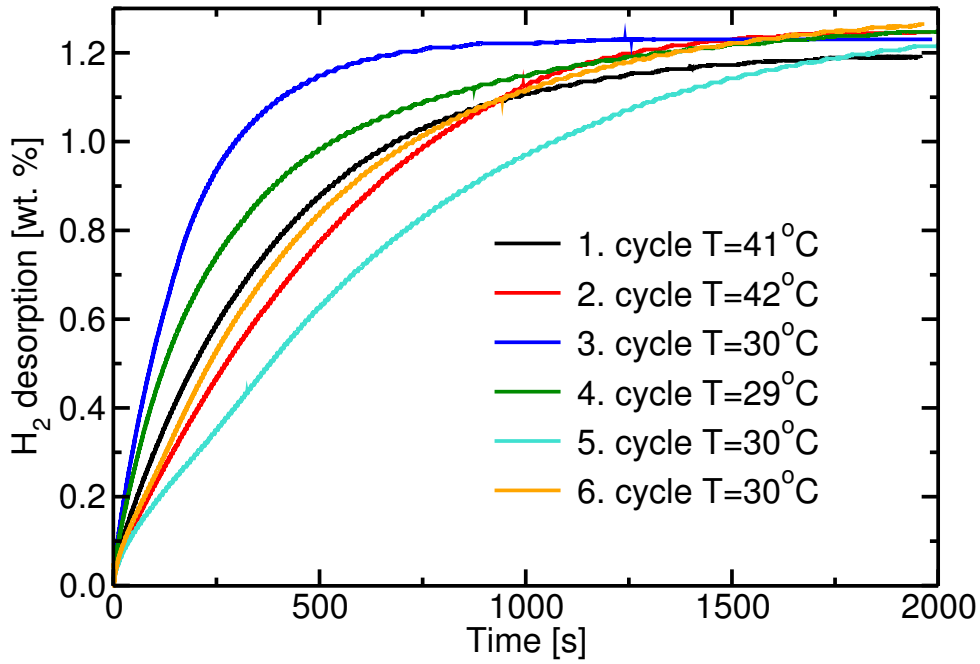

Figure 34: Hydrogen desorption from $LaNi_5$ at 0-1 bar hydrogen.

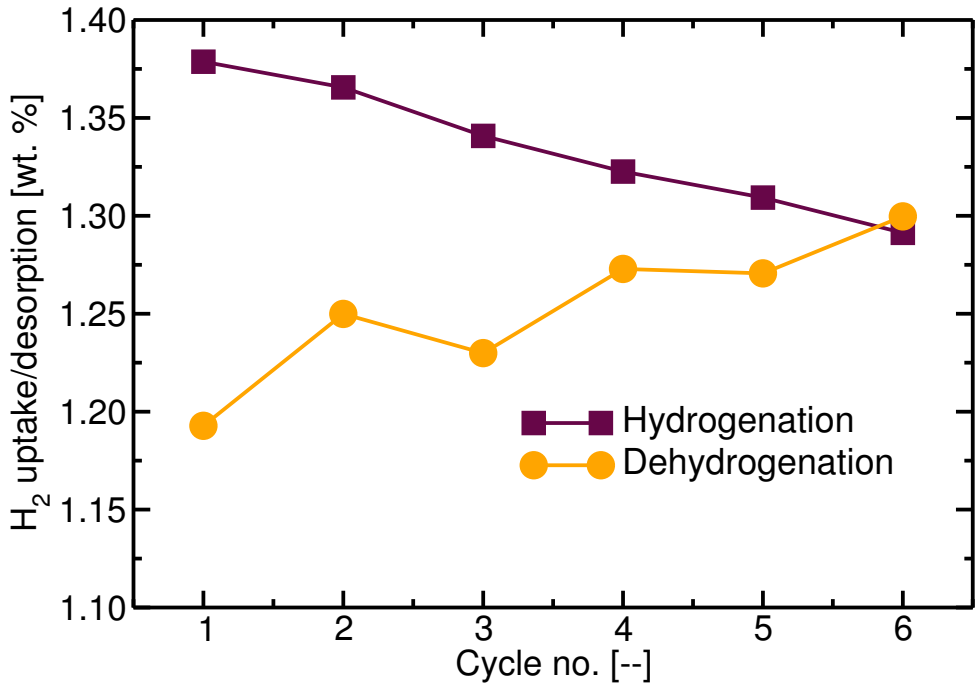

Figure 35: Hydrogen uptake and desorption, respectively, for $LaNi_5$ as a function of cycle number. In cycle 1-3 the initial hydrogen reactor pressure for hydrogenation is at vacuum level (approx. 10^{-2} mbar). In cycle 4-7 the initial pressure is increased to approx. 1 bar.

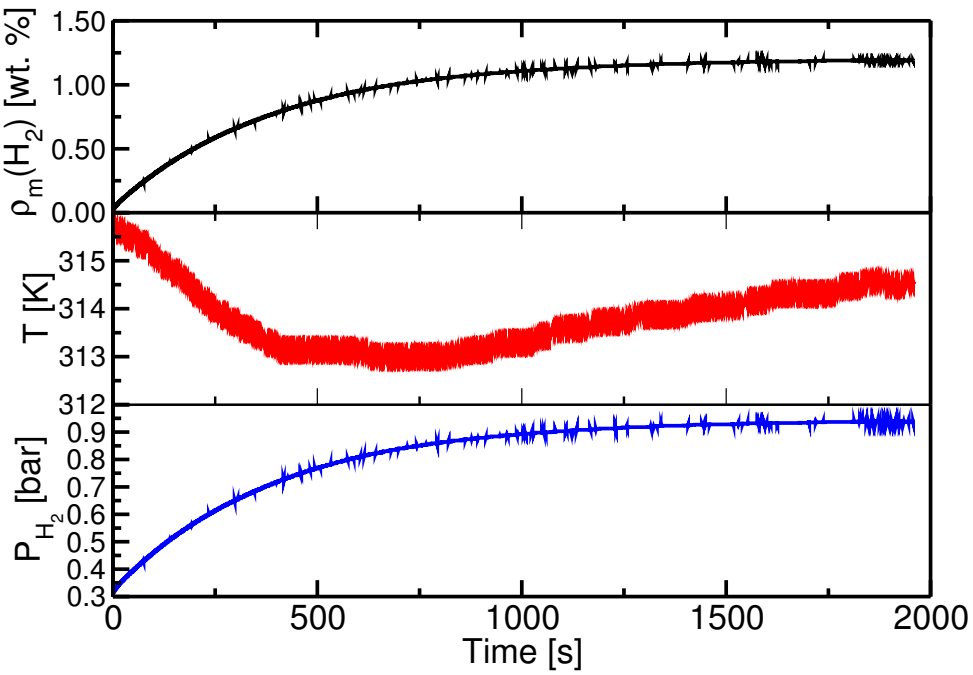

Figure 36: Hydrogen desorption, temperature and pressure for 1. cycle desorption from $LaNi_5$.

activation energy for desorption is higher than for absorption the rate is more sensitive to temperature variations. As for hydrogenation we observe significant temperature variations in the reactor during dehydrogenation cf. figure 36.

7.4 Determination of thermodynamic parameters

The new setup have also been used to measure Pressure-Composition-Isotherms for $LaNi_5$ at different temperatures in order to check its capabilities with respect to determining thermodynamic parameters.

Figure 37 (left) shows three PCI's at a temperature of 27 °C, 63 °C, and 90 °C, respectively. As expected the plateau pressure increases with increasing temperatures. However, comparing figure 37 with the data taken on the the old setup (high pressure balance, figure 6) we note that the plateaus measured on the new setup have a more sloping character, especially at elevated temperatures. This might be due to a gradual heat up of the hydride bed when hydrogen is absorbed by $LaNi_5$. For instance the temperature rose from 62.25 to 64.3 °C during the acquisition of the middle isotherm. This might at least partially account for the observed sloping. This suggests that a longer acquisition time should be utilized in order for the temperature to return to the starting temperature thus resulting in less sloping.

Figure 37 (right) shows the corresponding Van't Hoff plot of the isotherms in figure 37 (left). For comparison both data from the high pressure balance and literature data are included. From the figure there is apparently agreement between the data obtained on the new setup and the data included for comparison. A formation enthalpy of -27.5 kJ/mol is found for $LaNi_5H_6$ and a corresponding entropy change upon hydrogenation of -100 J/(mol K) is found. This agrees fairly well with the data of Lundin et al. [6] who finds -30.8 kJ/mol and -108 J/(mol K), respectively.

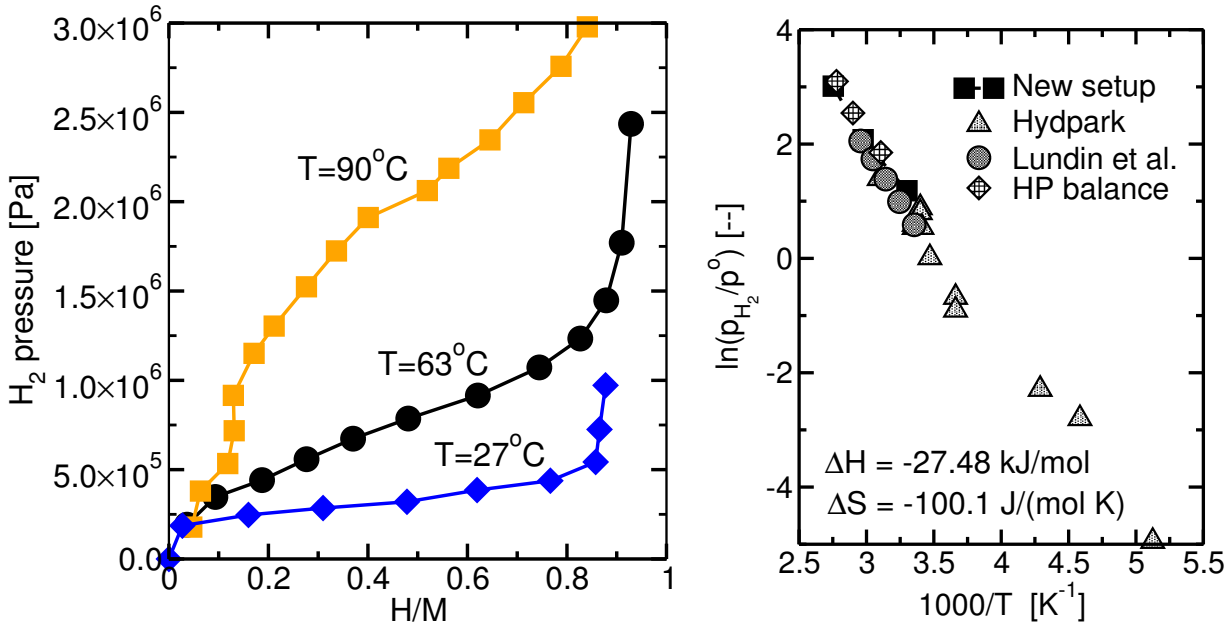

Figure 37: Left: Pressure-Composition-Isotherms for $LaNi_5$ at three different temperatures determined in the new setup. Right: Van't Hoff plot of the plateau pressure midpoints from the PCI's to the left. For comparison data from the high pressure balance is included as well as data from the literature.

8 Summary and recommendations

In this report a new experimental setup for testing hydrogen storage materials have been described in detail. The setup have proven to be leak tight both at ambient conditions and at elevated temperatures and pressures. In order to check the performance of the setup test experiments with 20 g $LaNi_5$ have been carried out. The setup allows determination of hydrogen capacity and thermodynamic parameters with sufficient accuracy. However, rather inconsistent kinetics was observed for $LaNi_5$. This might suggest that the setup suffers from heat transfer limitations when the reaction with hydrogen is fast. It is likely that the setup can be used to investigate kinetics for materials reacting more slowly with hydrogen e.g. magnesium. This will be investigated in the future. At the moment the pressure controller still needs to be connected to the data acquisition system. In order to obtain more reliable temperature data a thermocouple may be inserted directly into the hydride bed. When significant improvements have been made to the experimental setup this report will be replaced with a new and updated version.

References

[1] L. Schlapbach, A. Züttel, Nature 414 (2001) 353–358.

[2] A. Züttel, Materials Today 9 (2003) 24–33.

[3] A. Züttel, Naturwissenschaften 91 (2004) 157–172.

[4] http://www.eere.energy.gov/hydrogenandfuelcells/hydrogen/storage.html, U. S. Department of Energy, Last checked april 2004.

[5] B. Vigeholm, Chemical energy storage based on metal hydrides, Tech. Rep. Risø-M-2608, Risoe National Laboratory, DK-4000 Roskilde, Denmark, (In Danish) (1989).

[6] C. E. Lundin, F. E. Lynch, Solid state hydrogen storage materials for application to energy needs, Tech. Rep. AFOSR-TR-76-1124, University of Denver, Denver, USA (1975).

[7] A. S. Pedersen, J. Kjøller, B. Larsen, B. Vigeholm, International Journal of Hydrogen Energy 8 (3) (1983) 205–211.

[8] A. S. Pedersen, K. Jensen, B. Larsen, B. Vigeholm, Journal of the Less-Common Metals 131 (1987) 31–40.

[9] B. Vigeholm, J. Kjøller, B. Larsen, A. S. Pedersen, Journal of the Less-Common Metals 89 (1983) 135–144.

[10] B. Vigeholm, K. Jensen, B. Larsen, A. S. Pedersen, Journal of the Less-Common Metals 131 (1987) 133–141.

[11] A. S. Pedersen, J. Kjøller, B. Larsen, B. Vigeholm, International Journal of Hydrogen Energy 10(12) (1985) 852–857.

[12] B. Bogdanović, M. Schwickardi, Journal of Alloys and Compounds 253-254 (1997) 1–9.

[13] A. Züttel, P. Wenger, S. Rentsch, P. Sudan, P. Mauron, C. Emmenegger, Journal of Power Sources 118 (2003) 1–7.

[14] B. Bogdanović, R. Brand, A. Marjanović, M. Schwichardi, J. Tölle, Journal of Alloys and Compounds 302 (2000) 36–58.

[15] H. Morioka, K. Kakizaki, S.-C. Chung, A. Yamada, Journal of Alloys and Compounds 353 (2003) 310–314.

[16] A. S. Pedersen, J. Kjøller, B. Larsen, B. Vigeholm, J. A. Jensen, International Journal of Hydrogen Energy 9(9) (1984) 799–802.

[17] B. Vigeholm, J. Kjøller, B. Larsen, A. S. Pedersen, International Journal of Hydrogen Energy 8(10) (1983) 809–817.

[18] T. Heilmann, Praktisk regulering og instrumentering, 3rd Edition, Heilmanns, 1998.

[19] G. Alefeld, J. Völkl (Eds.), Hydrogen in metals II, Vol. 29 of Topics in Applied Physics, Springer-Verlag, 1978.

[20] L. Schlapbach (Ed.), Hydrogen in Intermetallic Compounds II. Surface and dynamic Properties, Applications, Vol. 67 of Topics in Applied Physics, Springer-Verlag, 1992.

[21] O. Boser, J. Less-Common Met. 46 (1976) 91–99.

[22] K. S. Nahm, W. Y. Kim, S. P. Hong, W. Y. Lee, Int. J. Hydrogen Energy 17 (5) (1992) 333–338.

[23] A. Andreasen, T. Vegge, A. S. Pedersen, Journal of Physical Chemistry B Submitted.

Mission

To promote an innovative and environmentally sustainable technological development within the areas of energy, industrial technology and bioproduction through research, innovation and advisory services.

Vision

Risø's research **shall extend the boundaries** for the understanding of nature's processes and interactions right down to the molecular nanoscale.

The results obtained shall **set new trends** for the development of sustainable technologies within the fields of energy, industrial technology and biotechnology.

The efforts made **shall benefit** Danish society and lead to the development of new multi-billion industries.